

ABSTRACT

DESIGN AND OPTIMIZATION OF 2012 FORMULA SAE CHASSIS WITH FINITE ELEMENT ANALYSIS FOR CSULB

By

Syed Naveed Hasan

December 2012

This work is a contribution to the design and optimization of a Formula SAE chassis for CSULB. A 3D CAD model of the previous chassis for CSULB was produced and modified to make it as rigid and lightweight as possible. The modified chassis was checked for static analysis using FEM as per SAE guidelines. Torsional stiffness of the structure was calculated by applying loads on suspension attachment points. The response of the structure under different load-cases and boundary conditions was analyzed on NX. The differences in the results were observed using 1D Beam and 2D Shell Elements. As an important design feature, five eigenvectors were calculated and the animations were shown, to study the overall dynamic behavior of the structure. Finally, an optimization was performed in order to maximize the torsional stiffness and minimize the chassis weight by minimizing tube thicknesses for different frame members avoiding failure in any loading condition.

DESIGN AND OPTIMIZATION OF 2012 FORMULA SAE CHASSIS WITH FINITE
ELEMENT ANALYSIS FOR CSULB

A THESIS

Presented to the Department of Mechanical and Aerospace Engineering
California State University, Long Beach

In Partial Fulfillment
of the Requirements for the Degree
Master of Science in Mechanical Engineering

Committee Members:

Christiane Beyer, Ph.D. (Chair)
Ortwin Ohtmer, Ph.D.
Tsair-Jyh Tzong, Ph.D.

College Designee

Burkhard Englert, Ph.D.

By Syed Naveed Hasan

B.E., 2007, NED University of Engineering and Technology

December 2012

UMI Number: 1522228

All rights reserved

INFORMATION TO ALL USERS

The quality of this reproduction is dependent upon the quality of the copy submitted.

In the unlikely event that the author did not send a complete manuscript and there are missing pages, these will be noted. Also, if material had to be removed, a note will indicate the deletion.



UMI 1522228

Published by ProQuest LLC (2013). Copyright in the Dissertation held by the Author.

Microform Edition © ProQuest LLC.

All rights reserved. This work is protected against unauthorized copying under Title 17, United States Code



ProQuest LLC.
789 East Eisenhower Parkway
P.O. Box 1346
Ann Arbor, MI 48106 - 1346

Copyright 2012

Syed Naveed Hasan

ALL RIGHTS RESERVED

ACKNOWLEDGEMENTS

I am heartily thankful to my supervisor, Dr. Christiane Beyer, whose encouragement, guidance and support from the initial to the final level enabled me to develop an understanding of the subject. Her invaluable help of constructive comments and suggestions throughout the simulation and report writing have contributed to the successful completion of this thesis.

I am also thankful to thesis committee members Dr. Ohtmer, Dr. Tzong and college designee Dr. Englert who responded well to review this report in a timely manner, enabling me to complete thesis on time.

Sincere thanks to all of the SAE team members at CSULB for showing several tips and ideas for chassis design, for running the entire SAE club, for fabrication of chassis, for design, manufacturing and assembling of Formula Race Car and finally for taking part in the competition in 2012.

Last but not least, my deepest gratitude goes to my beloved parents; Mr. and Mrs. Syed Razi Hasan and also to my brothers and sisters for their endless love, prayers and encouragement. To those who indirectly contributed in this thesis, your kindness means a lot to me. Thank you very much!

Syed Naveed Hasan

TABLE OF CONTENTS

	Page
ACKNOWLEDGEMENTS	iii
LIST OF TABLES	vi
LIST OF FIGURES	vii
LIST OF ABBREVIATIONS AND SYMBOLS	x
CHAPTER	
1. PLANNING AND CLARIFICATION	1
1.1. Introduction	1
1.2. Motivation	3
1.3. Procedure	4
1.3.1. Modeling in SolidWorks	4
1.3.2. Frame Manufacturability	6
1.3.3. Modeling in NX	8
2. CONCEPTUAL DESIGN	11
2.1. Concept of Round Suspension Attachment Members	11
2.2. Radius Elimination and Aerodynamics	13
2.3. Straight Suspension Attachment Members	13
2.4. Triangulation and Cross Bracings	14
2.5. Front Cradle Expansion	16
3. EMBODIMENT DESIGN	18
3.1. Front Roll Hoop	20
3.2. Main Roll Hoop, Bracing and Bracing Support	23
3.3. Side Impact Structure	25
3.4. Front Bulkhead & Bulkhead Support	28
3.5. Shoulder Harness Attachment	28
3.6. Torsional Stiffness Test	30
3.7. Dynamic Analysis	37

CHAPTER	Page
4. OPTIMIZATION	41
4.1. K/W Method	41
4.2. Geometry Optimization Via NX-8.....	43
4.2.1. Step 1	46
4.2.2. Step 2	50
4.2.3. Step 3	53
4.3. Final Observation.....	57
5. FINAL DESIGN	58
5.1. Roll Hoops	60
5.2. Main Hoop Bracings	61
5.3. Front Hoop Bracings.....	61
5.4. Front Bulkhead.....	62
5.5. Side Impact Structure.....	62
5.6. Shoulder Harness Attachment Member	62
5.7. Rear Cradle	63
5.8. Tertiary Members.....	63
5.9. Overall Details	63
6. CONCLUSION.....	66
REFERENCES	68

LIST OF TABLES

TABLE	Page
1. Properties of AISI-4130 Steel.....	19
2. Torsional Stiffness Calculation.....	34
3. Displacement Results For Simulations With Different Tube Thicknesses.....	42
4. Von-Mises Stress Results For Simulations With Different Tube Thicknesses.	42
5. Nodal Rotation and Torsional Stiffness Values.....	44
6. Optimization Via NX, Step 1.....	47
7. Optimization Via NX, Step 2.....	50
8. Optimization Via NX, Step 3.....	54
9. Space Frame Chassis Compartments Description.	60
10. CSULB FSAE 2012 General Details.....	63

LIST OF FIGURES

FIGURE	Page
1. 3D sketch of half of chassis in SolidWorks.....	5
2. Solid model of half of the chassis.....	6
3. Primary (red), secondary (blue) and tertiary (green) members.....	7
4. Tube notch profile.....	7
5. Pipe end treatments (trim and extend).....	8
6. Some of the available element types in NX-7.5.	10
7. Main roll hoop curvature modeled by 1D beam elements (left) and 2D shell elements (right).	10
8. Existing chassis design, isometric view.....	12
9. Existing chassis design, side view.	12
10. Round suspension attachment members.	13
11. Radius elimination and aerodynamically shaped chassis, option 1.	14
12. Existing chassis (top), option 1 (center), option 2 (bottom).	15
13. Straight suspension attachment members, option 2.....	16
14. Front cradle expansion.....	17
15. Finite element analysis steps.....	19
16. FE model geometry for different simulations.....	20
17. Deflection and Von-Mises stress distributions of chassis with 1D elements.	21
18. Deflection and Von-Mises stress distributions of chassis with 2D elements.	21

FIGURE	Page
19. Additional tubes for front roll hoop support.	23
20. Deflection and Von-Mises stress distributions of chassis with 1D elements.	24
21. Deflection and Von-Mises stress distributions of chassis with 2D elements.	24
22. Location of maximum stress at joint (shown in red) for 2D element.	25
23. FE model for side impact structure simulation.	25
24. Deflection and Von-Mises stress distributions of chassis with 1D elements.	26
25. Deflection and Von-Mises stress distributions of chassis with 2D elements.	27
26. Location of four joints with Von-Mises greater than 26016 psi.	27
27. Location of load for front bulkhead.	28
28. Deflection and Von-Mises stress distributions of chassis with 1D elements.	29
29. Deflection and Von-Mises stress distributions of chassis with 2D elements.	29
30. Deflection and Von-Mises stress distributions of chassis with 1D elements.	30
31. Deflection and Von-Mises stress distributions of chassis with 2D elements.	31
32. Front suspension load application points.	33
33. Rear suspension fixed constraints.	33
34. Nodal rotation distribution for torsional load case 1.	35
35. Nodal rotation distribution for torsional load case 4.	35
36. Nodal rotation distribution for torsional load case 7.	36
37. Nodal rotation distribution for torsional load case 10.	36
38. FE model showing simply supported constraints at front suspension.	37
39. FE model showing fixed constraints at rear suspension.	38
40. Nodal displacement results for mode 1 and mode 2.	38

FIGURE	Page
41. Nodal displacement results for mode 3 and mode 4.....	39
42. Nodal displacement results for mode 5.....	39
43. Objective function graph for step 1.	47
44. First constraint graph for optimization step 1.....	48
45. Second constraint graph for optimization step 1.....	48
46. Third constraint graph for optimization step 1.	49
47. Fourth constraint graph for optimization step 1.....	49
48. Objective function graph for optimization step 2.	51
49. First constraint graph for optimization step 2.....	51
50. Second constraint graph for optimization step 2.....	52
51. Third constraint graph for optimization step 2.	52
52. Fourth constraint graph for optimization step 2.....	53
53. Objective function graph for optimization step 3.	54
54. First constraint graph for optimization step 3.....	55
55. Second constraint graph for optimization step 3.....	55
56. Third constraint graph for optimization step 3.	56
57. Fourth constraint graph for optimization step 3.....	56
58. Final design.....	58
59. 2012 CSULB FSAE showing general dimensions (top view).....	59
60. 2012 CSULB FSAE showing general dimensions (front view).....	60
61. Important dimensions complying with FSAE Rules 2012.	65

LIST OF ABBREVIATIONS AND SYMBOLS

CSULB	California State University Long Beach
SAE	Society of Automotive Engineers
FSAE	Formula Series Vehicle, Society of Automotive Engineers
FE model	Finite Element model
CAD	Computer Aided Design
CAM	Computer Aided Manufacturing
θ	Nodal rotation in y-direction or along length of chassis
T	Torsion
L	Torsion arm
K	Torsional stiffness
I.R.	Internal radius of tube
E	Young's Modulus (Modulus of elasticity)
G	Shear Modulus
ν	Poisson's ratio
ρ	Density
1D	One dimensional
2D	Two dimensional
F _x	Force applied in x-direction
F _y	Force applied in y-direction

Fz	Force applied in z-direction
FEM	Finite Element Method
NX	A CAD/CAM software package developed by Siemens PLM Software

CHAPTER 1

PLANNING AND CLARIFICATION

1.1. Introduction

The Formula SAE Series is a student design competition organized by SAE International that challenges teams of university students to conceive, design, fabricate, develop and compete with small, formula style, vehicle.

The basic concept behind Formula SAE is that a design firm has contracted teams to design, fabricate, test and demonstrate a prototype vehicle for non-professional, weekend, autocross competition market.

This study shows the design stages underwent by CSULB SAE team for design of their formula chassis for 2012 competition. The design process was initiated by modeling the existing chassis from previous competition on SolidWorks, modifying this design in order to comply with the updated SAE rules for 2012 competition and make the chassis rigid in order to avoid large deflections and failures in an event of crash or roll-over. This thesis also shows how to validate the strength requirements of a typical formula chassis, how to estimate torsional stiffness of the designed chassis without fabricating equipments to check the stiffness and how to optimize the frame to make it rigid and lightweight.

The Formula Series is dictated by a set of rules set in place to ensure the safety of vehicles and competition. For chassis design, the key rules include protection of front

bulkhead and side impact structure including rollover protection. The rules suggest main and front roll hoops to be made of 1” outer diameter steel tubing with 0.095” minimum wall thickness. Side impact structure, front bulkhead, supports and bracings must be constructed of 1” outer diameter steel tubing with either 0.065” or 0.049” wall thickness, depending on the type of bracing. Though these materials are stated in the rules, the competition allows for approved alternatives such as composite materials.

A good race car chassis design should meet certain requirements that include, but are not limited to, light weight, high torsional stiffness and flexural rigidity, optimum suspension geometry, driver safety, low center of gravity, etcetera, in order to have good drivability and maneuverability.

In order to construct a competitive Formula-SAE vehicle, the car needs to be fuel efficient and reasonably priced in addition to being fast. The key factor is to get a good balance between efficient suspension and frame designs, reliability of the components used, and driver friendly engine torque features. So all parts of the 2012 CSULB FSAE were designed to be simple and easy to manufacture with good performance balance and low production and maintenance cost.

This work focuses on evaluating the chassis strength to withstand forces acting on the frame for design conditions, minimizing weight and to assessing the torsional stiffness of the chassis before fabrication so that chassis design may be modified if required to maximize torsional stiffness. Since this structure has a complex geometry, some difficulties were encountered to find out optimal design using analytical formulation which would be addressed in the later section.

1.2. Motivation

The development of sports cars awakened the interest of many enthusiastic and specialists in the automobile area during the last few decades. Consequently, their demand motivated the competition between manufacturers from all over the world to dominate international markets. Therefore, Formula SAE competition offers teams of university students to practically take part in the world competition. The key factors to compete in international sports car markets are high performance, well weight/power ratio, good drivability, maneuverability and stability conditions, comfort and security.

The above mentioned factors are highly dependent upon a well-designed chassis. Thompson et al. in their work [1] concluded that each structural member of a chassis exerts a certain influence in its torsional stiffness. Happian in his research [2] also emphasized that the torsional stiffness of a chassis is the major factor for maneuverability and drivability. The torsional stiffness guarantees the vehicle structural integrity and its general behavior.

One of the advantages that space frames structures offer over monocoque is that they are easy to manufacture. Space frames simply consist of an arrangement of structural members stressed primarily in tension and compression like a 3D truss. They offer lightweight, high torsional stiffness, and security for occupants.

To achieve a rigid and lightweight structure is the objective of a sports car design. De Oliveira and Borges stated in their work [3] that the most effective strategy should consider both the weight reduction and the increase of torsional stiffness. So material and geometric properties including density, Young's modulus, moment of inertia, total weight, center of gravity and a high torsional stiffness play vital roles in structure design.

1.3. Procedure

The procedure for 2012 chassis design for CSULB consisted of producing a 3D model of previous chassis on SolidWorks and making certain design changes in order to fulfill updated competition rules. After that different conceptual design changes were done in order to make the chassis torsionally stiff. 3D modeling of updated chassis was produced in NX for simulation. Advanced simulation was done on NX with load cases and boundary conditions according to SAE guidelines for 2012 competition [4] in order to predict the extent of safety for the frame under roll-overs and crashes. Finally, the magnitude of torsional stiffness was determined.

The frame modeling in SolidWorks and in NX is described in this chapter, whereas conceptual design changes are described in chapter 2, advanced simulation and torsional stiffness tests are performed in chapter 3, optimization is performed in chapter 4 and then a brief explanation of final chassis design is given in chapter 5.

1.3.1. Modeling in SolidWorks

The first step to model chassis in SolidWorks was to start from a 3D Sketch. Due to the symmetric nature of frame, only left half was drawn using lines, arcs and fillets as shown in figure 1. After creating the 3D sketch, weldment was used to create 3D structural members of half frame as shown in figure 2. The solid bodies created thru weldment can be “Trimmed and Extended” at the joints whereas the solid bodies created thru “Extrude” or “Sweep” cannot be trimmed and extended at the joints. “Trim and Extend” command was used to remove the sharp edges and extended portion of members at joint location.

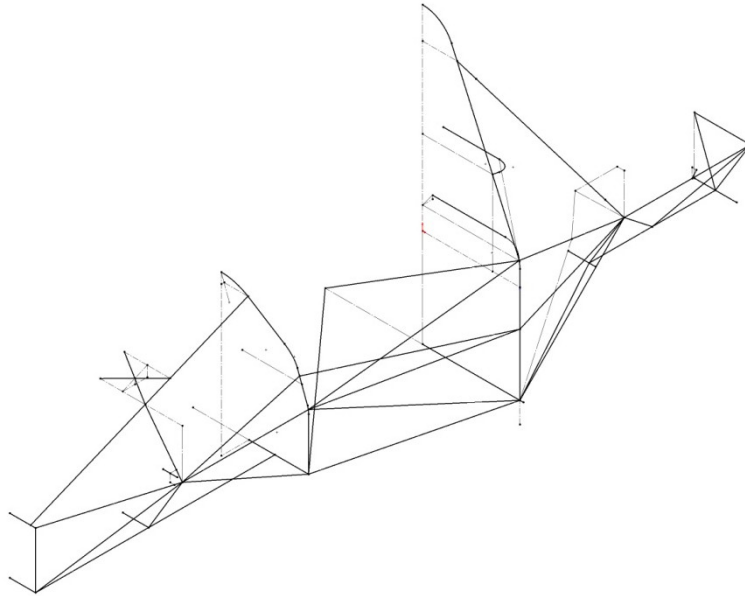


FIGURE 1. 3D sketch of half of chassis in SolidWorks.

Three types of tube sections were used for weldment:

- 1) Outer Diameter 1", Wall Thickness 0.12"
- 2) Outer Diameter 1", Wall Thickness 0.65"
- 3) Outer Diameter 0.5", Wall Thickness 0.65"

First type is used primarily for the cockpit of the chassis where high strength is required for driver's safety as shown by red color in figure 3. Second type of tube was used to create remaining frame members except the connecting members for triangulation as shown by blue color in figure 3. Third type of tube was used to create connecting members for triangulation of the frame as shown by green color in figure 3. Using mirror command about right plane, the entire chassis model was created as shown in figure 3.

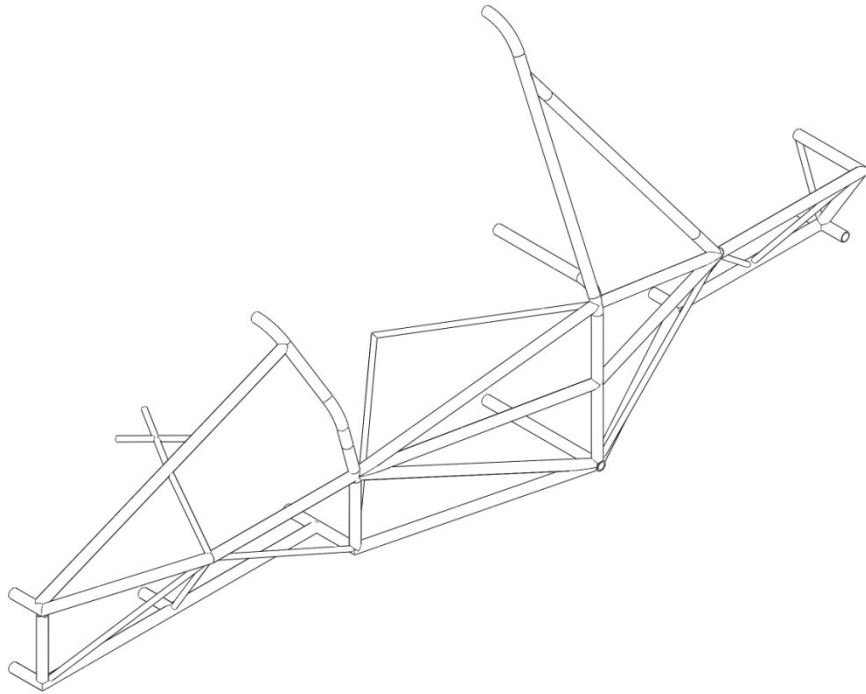


FIGURE 2. Solid model of half of the chassis

1.3.2. Frame Manufacturability

The 3D model created in SolidWorks was used to create Flat Pattern Sheet Metal of each structural member. These flat pattern were used for the notch profiles at each joint for helping the fabrication of these members. An example of notch profile of one the members of rear bulkhead is shown in figure 4.

The goal of the frame design was to achieve high reliability, low cost and high adjustability. For that purpose, pipe ends were treated to have cuts perpendicular to its length before welding as shown in figure 5. These notch profiles reflected in the SolidWorks CAD drawings were used to wrap around actual pipe end and grind to have the same shape as present in the drawing.

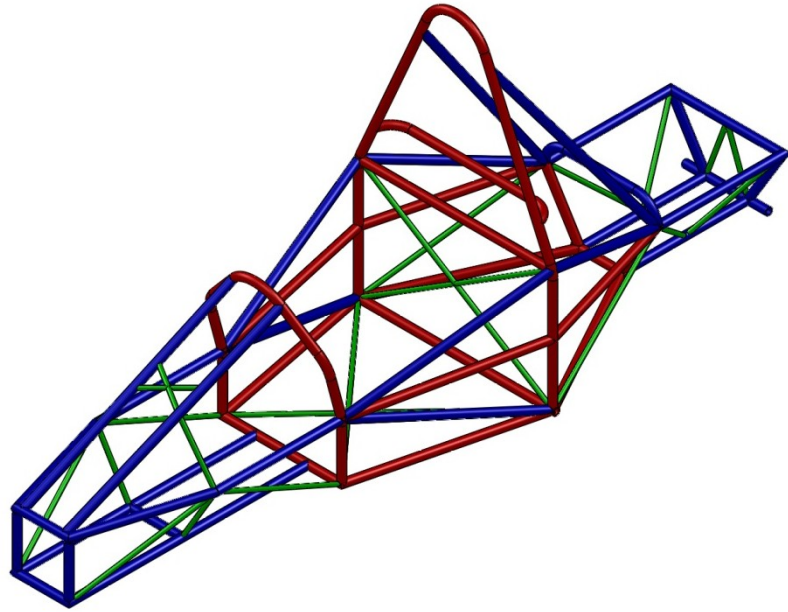


FIGURE 3. Primary (red), secondary (blue) and tertiary (green) members.

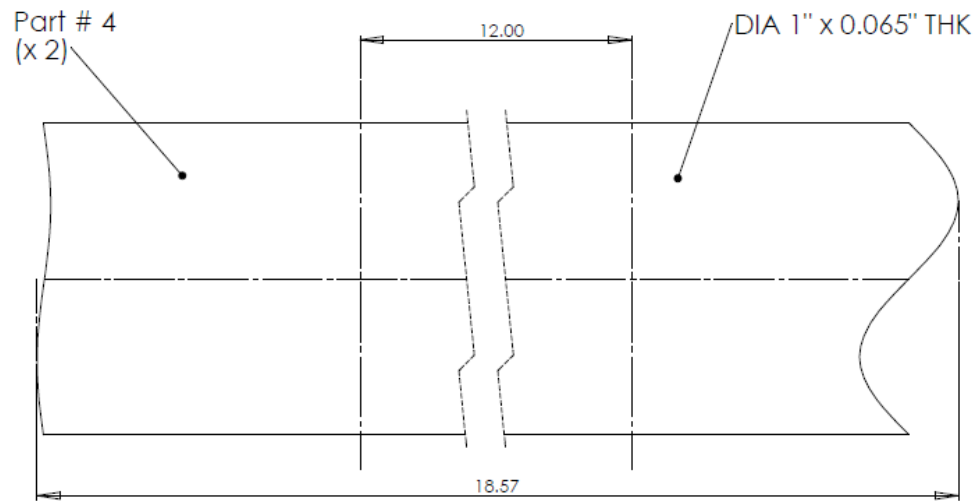


FIGURE 4. Tube notch profile.

This step was required due to the absence of laser pipe cutting machine. If laser pipe cutting machine was available these drawings could be fed, translated and directly processed which would allow an automated pipe end welding preparation process and decrease labor work.

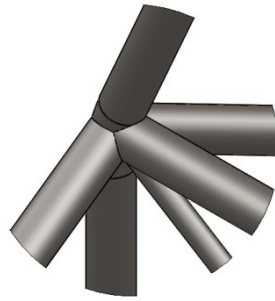


FIGURE 5. Pipe end treatments (trim and extend)

1.3.3. Modeling in NX

Structural analysis of the chassis was done in NX. Even SolidWorks and NX share same file formats such as IGES, STEP, PARASOLID, SLDPRT, the chassis geometry created by SolidWorks needs to be significantly cleaned up prior to be used by NX. Therefore, it was decided to model the chassis geometry in NX. The basic technique for modeling the frame in NX was the same as in SolidWorks, except the following:

- 1) Instead of creating one 3D sketch in SolidWorks, multiple sketches were created in NX on different planes for different members.

2) “Tube” command was used in NX instead of Weldment in SolidWorks. But this command could be used only for the single members or continuous members joined together with smooth tangent such as Main Roll Hoop.

3) “Swept” command was used in NX for creating members with Butt-Welded or sharp joints.

There are several options regarding the finite element modeling or meshing of such a structure. 1D beam elements produce models at lower computational cost, without losing the necessary accuracy in the design phase. 2D shell elements sometimes prove to be expensive solution from the computational point of view although they produce more accurate results. In addition, the 2D elements are not convenient to use to find the optimal chassis design. Some basic element types available in NX-7.5 that could be used for the chassis modeling are shown in figure 6. For the chassis design, two types of meshing were used to create a finite element model.

- 1) 1D CBEAM Element with physical properties as PBEAM.
- 2) 2D CQUAD4 Element with physical properties as PSHELL.

The 1D beam element PBEAM has just two nodes and requires user to input element length and element cross section. Moreover, this element can be defined by meshing a line and no surface or solid modeling is required. This element can be used in the analysis of tension, compression, torsion and bending. Each element has twelve degrees of freedom, i.e., three translations and three rotations for each node.

2D beam element CQUAD4 with PSHELL physical properties has four nodes with six degrees of freedom at each node (three translations and three rotations). Unlike 1D beam element, 2D shell element cannot be created on a line. Instead it requires

surface on which it can be meshed. Although it needs more modeling steps than 1D element, it can be used on the joints to represent the joint shape better than 1D beam element. Moreover, 2D shell elements approximate a curved beam or any curved surface better than 1D beam element as shown in figure 7.

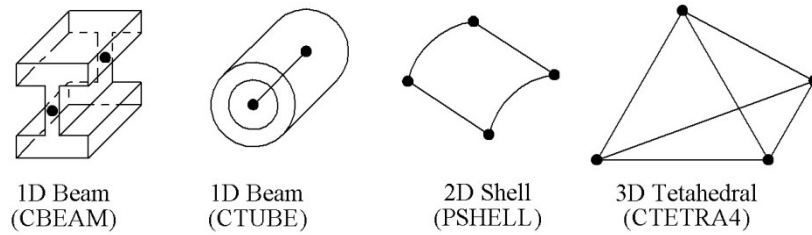


FIGURE 6. Some of the available element types in NX-7.5.



FIGURE 7. Main roll hoop curvature modeled by 1D beam elements (left) and 2D shell elements (right).

CHAPTER 2

CONCEPTUAL DESIGN

The main purpose of the designed chassis is to rigidly connect the front and rear suspension while providing attachment points for the different systems of the car. The design team at California State University Long Beach started FSAE chassis design with the existing chassis from previous competition that needed several modifications in order to take part in the competition. The existing design from previous competition is shown in figure 8 and figure 9. This chassis has tubular space-frame style which consists of a series of tubes which are joined together to form a structure that connects the necessary components together.

2.1. Concept of Round Suspension Attachment Members

The existing chassis had square shaped tubular members where suspension arms are mounted as shown in figure 8. These were changed to round tubes in the new design as shown in figure 10. This was done because round shape of 1 inch diameter has less weight as compared to 1 inch square tube of same thickness. Round tube could be bent easily in any direction and was also cheaper than square tubes. So, it was better suited for space frame chassis.

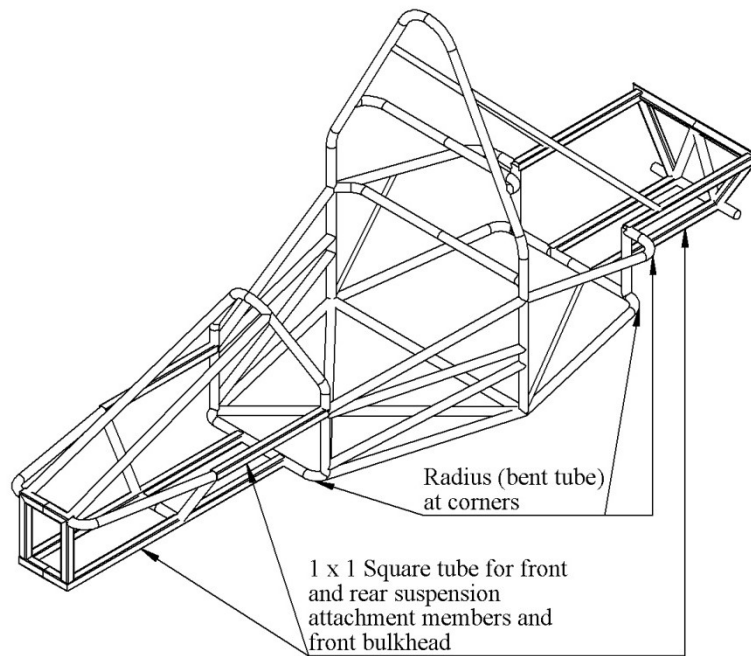


FIGURE 8. Existing chassis design, isometric view.

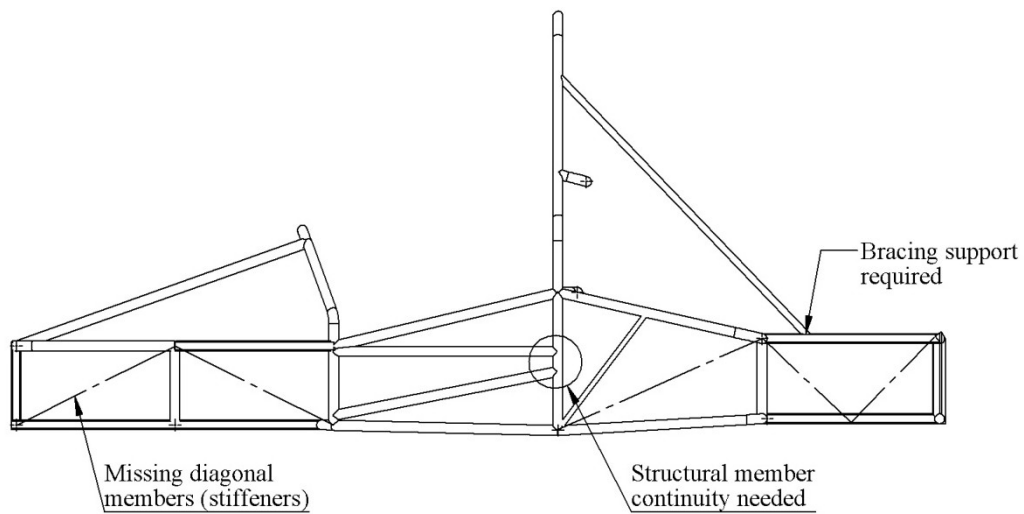


FIGURE 9. Existing chassis design, side view.

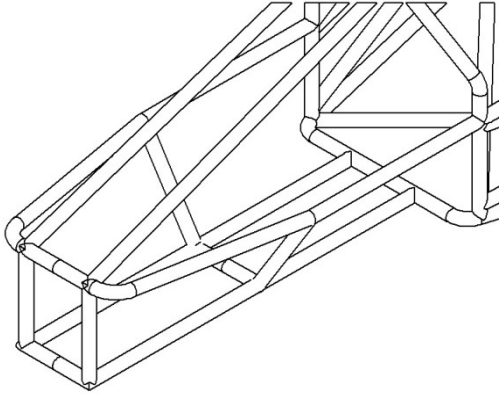


FIGURE 10. Round suspension attachment members.

2.2. Radius Elimination and Aerodynamics

Effort was made in modifying some aerodynamic shape of the chassis as shown in figure 11. However, some portion of this shape was brought back to the original state for ease of manufacturing and to have straight members for suspension arm support.

2.3. Straight Suspension Attachment Members

Whenever a bent tube is used it must be supported or reinforced at the beginning and end of the curved section in order to get better strength to resist design loads. The existing chassis had curved sections at the bottom of cockpit and near engine location as shown at top in figure 12. To remove that, the first option was to create inclined members as shown at the middle of the same figure. Second was to have straight suspension attachment members and the rest inclined as shown at the bottom of that figure and in figure 13. Since the first option needed much complex calculations for suspension operation because of unequal suspension arms, the second option was chosen.

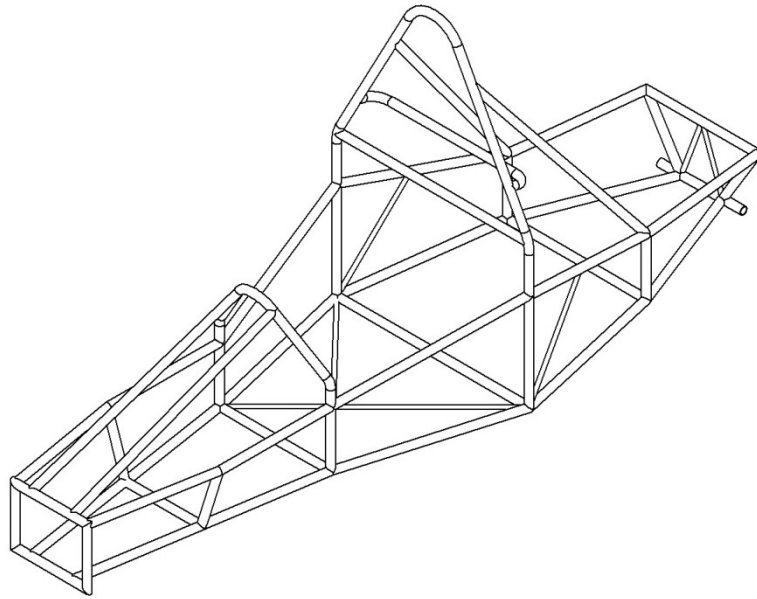


FIGURE 11. Radius elimination and aerodynamically shaped chassis, option 1.

2.4. Triangulation and Cross Bracings

Triangulation is used to increase the torsional stiffness of a frame as shown in figure 3. The concept behind triangulation is the same as it is for trusses. Trusses are composed of triangles because of the structural stability of that shape and design. A triangle is the simplest geometric figure that will not change shape when the lengths of the sides are fixed. In comparison, both the angles and the lengths of a four-sided figure must be fixed to retain its shape. An effort was made to triangulate the chassis as much as possible. The triangular shape is the basic geometric form that guarantees a high torsional stiffness. The use of diagonal bars (stiffeners) is a good option to get a rigid 3D structure, according to Adams [5]. The triangular regions appearance in the chassis and in a typical truss structure is the result of this use.

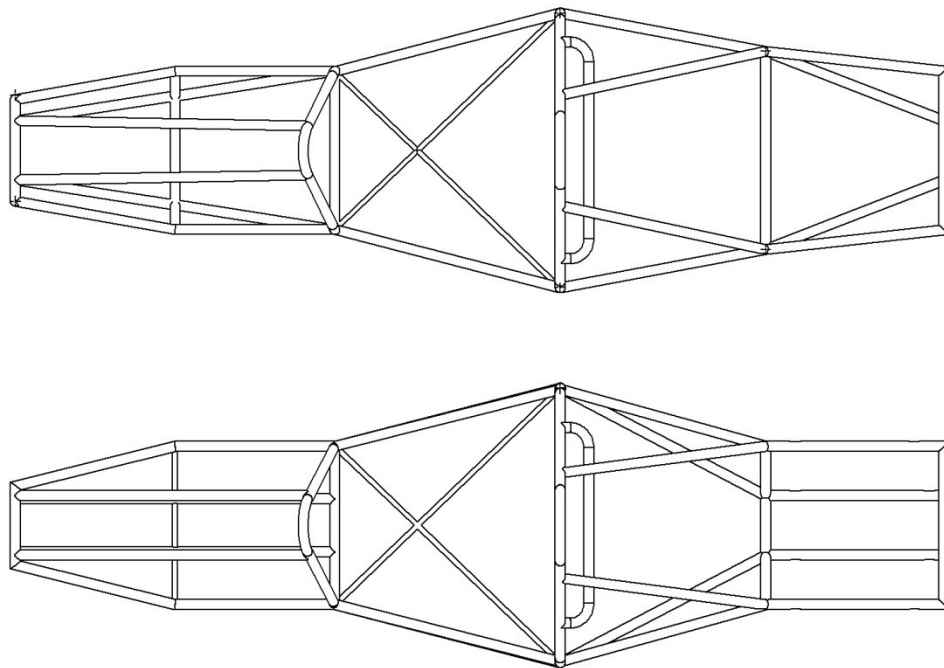
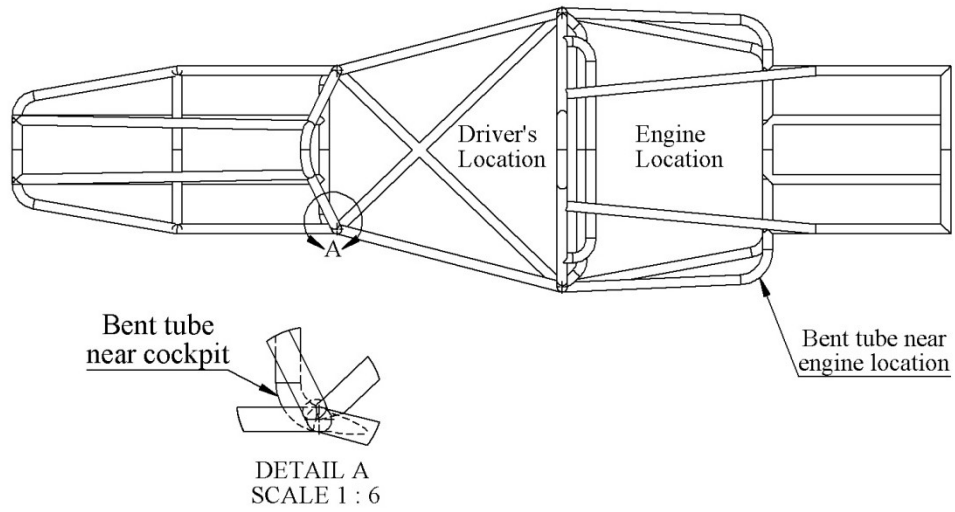


FIGURE 12. Existing chassis (top), option 1 (center), option 2 (bottom).

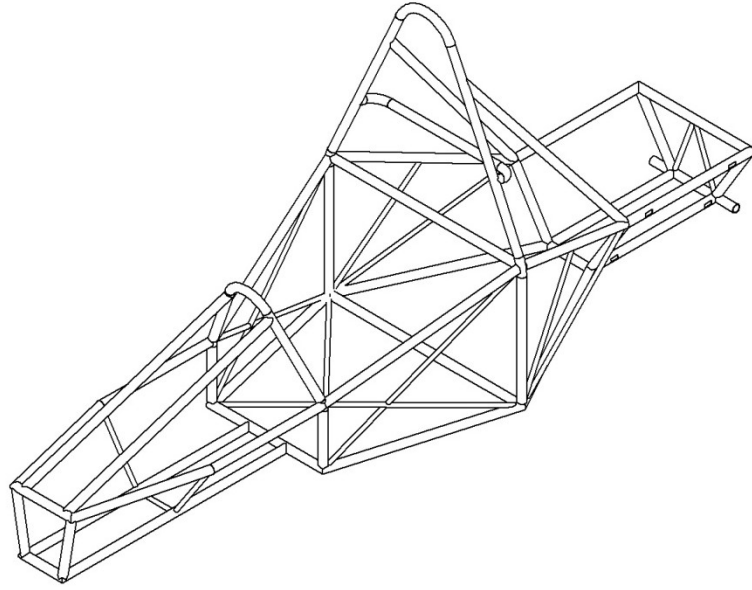


FIGURE 13. Straight suspension attachment members, option 2.

The components which produce significant amounts of force, for example the engine and suspension, were attached to the frame at triangulated points. Previous CSULB frames have lacked adequate triangulation for highly loaded components as shown in figure 9. For the 2012 car, all of the highly loaded components were attached to triangulated points as shown in figure 3.

2.5. Front Cradle Expansion

Front roll hoop was raised 3 inches to make chassis ergonomically better for the driver's legs. The existing chassis was built tight and compact but was proved to be insufficient for ease of installation of steering wheel, brake pedals, rack and pinion assembly and other components in addition to have enough room for driver's legs. Furthermore, the bend location for front roll hoop was moved to the closest joint in order to get better load transfer and have good strength as shown in figure 14.

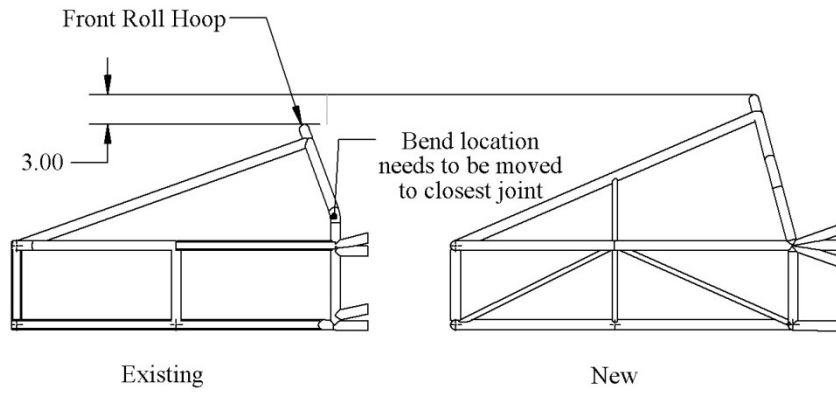


FIGURE 14. Front cradle expansion.

CHAPTER 3

EMBODIMENT DESIGN

With different factors in mind such as materials, strength, cost, fabrication time and availability of tools, the final design selected is given in figure 3. Frame members were positioned in the order of priority of suspension geometry, ease of construction and rigidity.

The use of Finite Element method is the most common approach to design a three-dimensional vehicular structure. Therefore, the improved design was used to run static analysis in NX to check for deformation and stresses and to verify whether they are within allowable limits or not. For this purpose, SAE guidelines [4] were used to define forces and boundary conditions for different load cases.

Simulation was done with 1D PBEAM and 2D CQUAD4 element types as described in section 1.3.3 and results were compared. The solution type was SESTATIC 101 in NX-7.5 for the simulations presented in sections 3.1 to 3.6. The material used was AISI 4130 whose properties were entered into NX. This was done by copying steel material in NX library and changing the parameters given in table 1.

Simulation steps are described in figure 15 and the FE model geometry for simulations presented in sections 3.1 to 3.5 is shown in figure 16.

TABLE 1. Properties of AISI-4130 Steel

Property	Value	Unit
Elastic Modulus (E)	205	GPa
Poisson's ratio (ν)	0.285	n/a
Shear Modulus (G)	80	GPa
Density (ρ)	7850	kg/m ³
Tensile Strength	731	MPa
Yield Strength	460	MPa
Thermal Conductivity	42.7	W/(m·K)
Specific Heat	477	J/(kg·K)

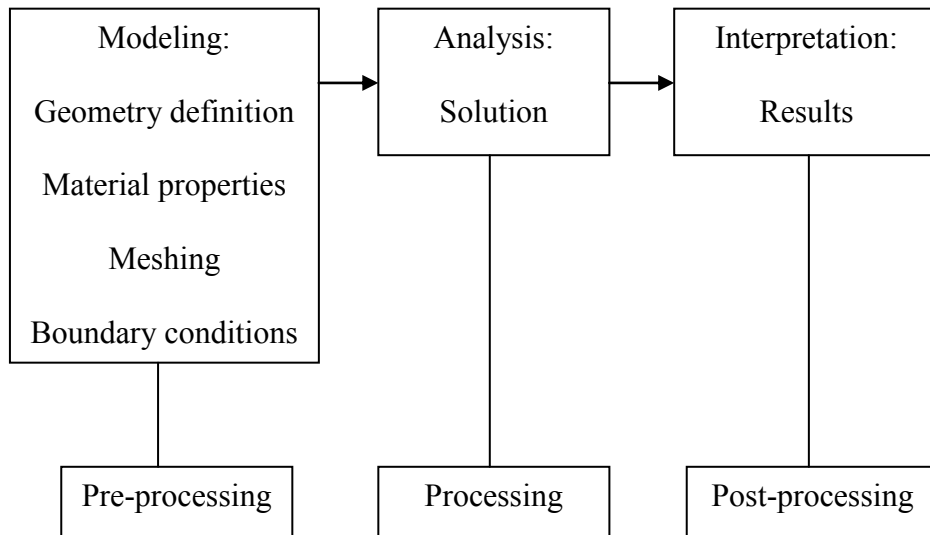


FIGURE 15. Finite element analysis steps.

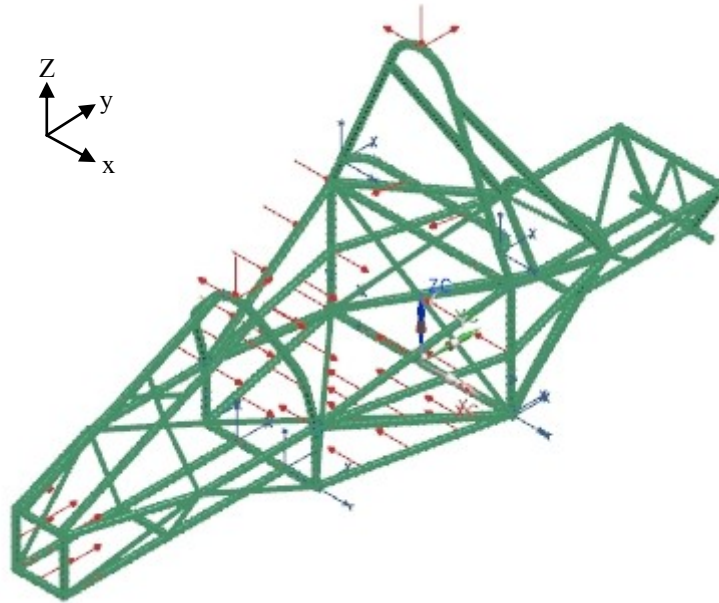


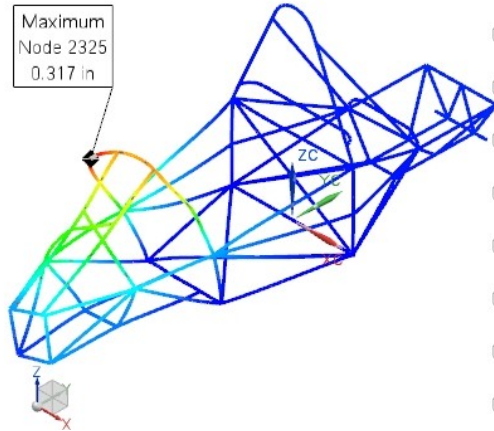
FIGURE 16. FE model geometry for different simulations.

3.1. Front Roll Hoop

Load applied: $F_x = -5.0$ kN, $F_y = 6.0$ kN, $F_z = -9.0$ kN. Application point: Top of front roll hoop. Boundary condition: Fixed displacement (x, y, z) but not rotation of the bottom nodes of both sides of the front and main roll hoops. Max allowable deflection: 1 inch.

Results are shown in figure 17 and figure 18. These results show the difference in maximum deformation and Von-Mises stress using beam and shell elements. The maximum deformation is 0.317 inches and 0.23 inches for beam and shell elements respectively. The location of maximum deformation is the same for either case. However, the location of maximum Von-Mises stress is different between the two cases. For beam elements, the maximum Von-Mises stress is 71533 psi at location where the front roll hoop bends without any joint or reinforcement.

13_sim2 : Front Roll Hoop Result
 Subcase - Static Loads 1, Static Step 1
 Displacement - Nodal, Magnitude
 Min : 0.000, Max : 0.317, Units = in
 Deformation : Displacement - Nodal Magnitude



13_sim2 : Front Roll Hoop Result
 Subcase - Static Loads 1, Static Step 1
 Stress - Element-Nodal, Unaveraged, Von-Mises
 Beam Section : Maximum
 Min : 0.00E+000, Max : 7.15E+004, Units = lbf/in²(psi) 7.15E+004
 Beam Coord sys : Local
 Deformation : Displacement - Nodal Magnitude

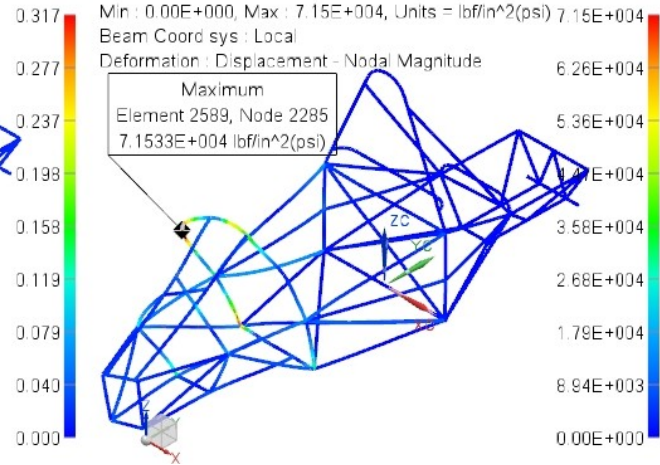
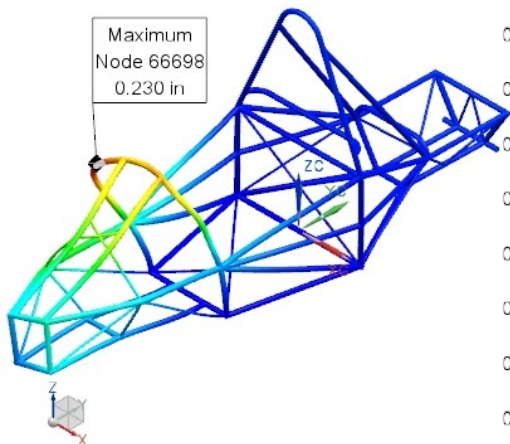


FIGURE 17. Deflection and Von-Mises stress distributions of chassis with 1D elements.

14_sim1 : Front Roll Hoop Result
 Subcase - Static Loads 1, Static Step 1
 Displacement - Nodal, Magnitude
 Min : 0.000, Max : 0.230, Units = in
 Deformation : Displacement - Nodal Magnitude



14_sim1 : Front Roll Hoop Result
 Subcase - Static Loads 1, Static Step 1
 Stress - Element-Nodal, Unaveraged, Von-Mises
 Shell Section : Top
 Min : 4.91E-010, Max : 8.76E+004, Units = lbf/in²(psi) 8.76E+004
 Deformation : Displacement - Nodal Magnitude

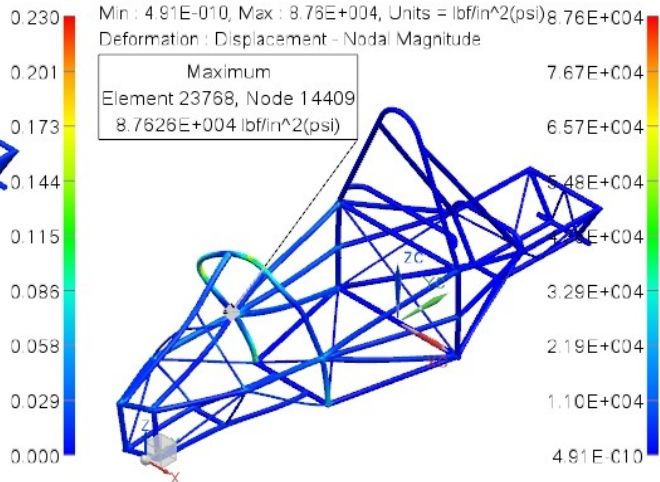


FIGURE 18. Deflection and Von-Mises stress distributions of chassis with 2D elements.

For shell elements, the maximum Von-Mises stress is 87626 psi at the joint just after the bend where stress level was maximum for beam elements. This is because shell element meshing was done on member surfaces that represent actual tube members and joints. It includes pipe end treatment details for the joints. The beam element meshing was done on lines that represent path of the tubes and no pipe-end treatment detail is incorporated in this type of mesh. 2D elements on curved or flat surfaces represent approximations, therefore a fine mesh is required. Straight 1D elements connected at the ends only, represent exact solutions, therefore a mesh is not required. However, the 2D elements require more time for modeling and analysis since the surface of the tube needs to be modeled first prior to meshing. For the purpose of optimization, a beam element is easier to handle because it doesn't require surface or solid modeling repeatedly while making changes to the size of tube. Since this study is more focused towards thickness selection of the tubes and optimization rather than concentrating on joint analysis, beam elements were used for most of the analyses in the remaining portion of this report.

Furthermore, the maximum Von-Mises stress is greater than yield strength of material which is 66717 psi. This means that front roll hoop is not safe under applied loading conditions. So additional members or gusset plate are required to provide necessary support for front roll hoop. Two additional tubes of diameter 0.5 inches and wall thickness 0.065 inches were used for this purpose at location where front roll hoop bends when looking from front of the chassis. These members are shown in figure 19. All of the remaining simulations were done with these added members and finally during optimization front roll hoop would be checked again for the induced stresses.

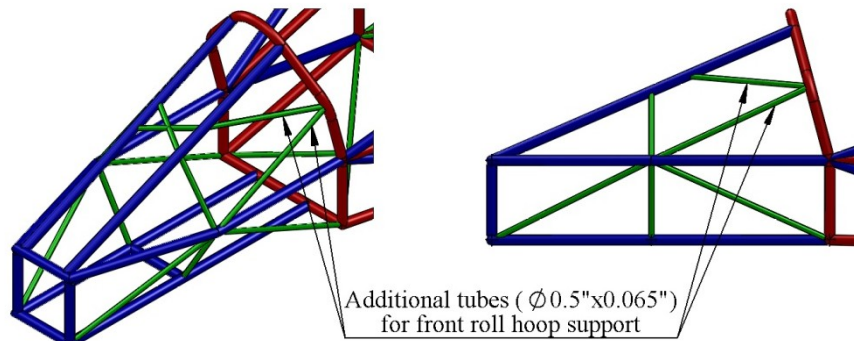


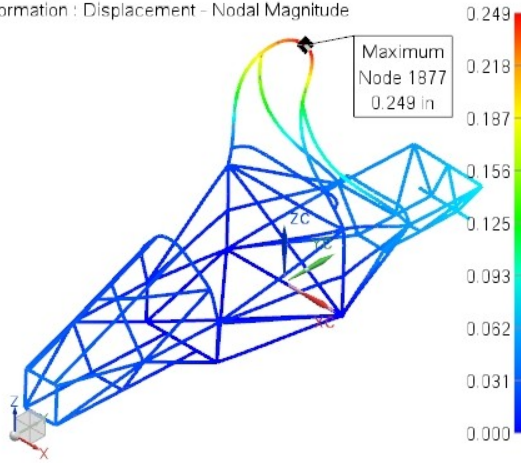
FIGURE 19. Additional tubes for front roll hoop support.

3.2. Main Roll Hoop, Bracing and Bracing Support

Load applied: $F_x = -5.0$ kN, $F_y = 6.0$ kN, $F_z = -9.0$ kN. Application point: Top of main roll hoop. Boundary condition: Fixed displacement (x, y, z) but not rotation of the bottom nodes of both sides of the front and main roll hoops. Max allowable deflection: 1 inch.

Simulation results are shown in figure 20 and figure 21. The maximum deformation is 0.249 inches and 0.244 inches for beam and shell elements respectively. The maximum Von-Mises stress is 54872 psi and 61472 psi for beam and shell elements respectively. These results also show that 2D element results have higher induced stresses. The location of maximum deformation and Von-Mises stress remains the same for either case. The location of maximum Von-Mises stress for 2D elements at the joint where main roll hoop connects with the bracing is shown in figure 22. The element with red color indicates the maximum stress.

13_sim2 : Main Roll Hoop Result
 Subcase - Static Loads 1, Static Step 1
 Displacement - Nodal, Magnitude
 Min : 0.000, Max : 0.249, Units = in
 Deformation : Displacement - Nodal Magnitude



13_sim2 : Main Roll Hoop Result
 Subcase - Static Loads 1, Static Step 1
 Stress - Element-Nodal, Unaveraged, Von-Mises
 Beam Section : Maximum
 Min : 0.00E+000, Max : 5.49E+004, Units = lbf/in²(psi)
 Beam Coord sys : Local
 Deformation : Displacement - Nodal Magnitude

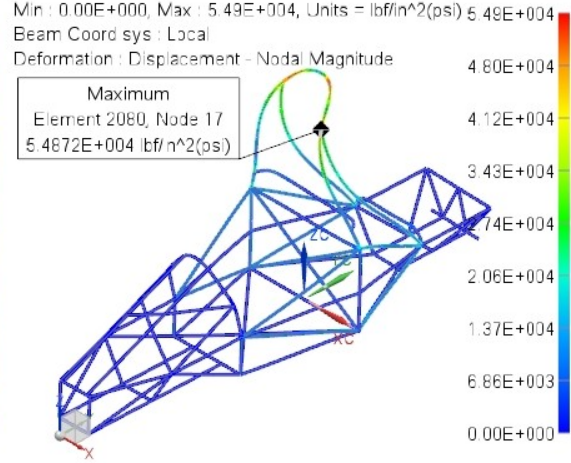
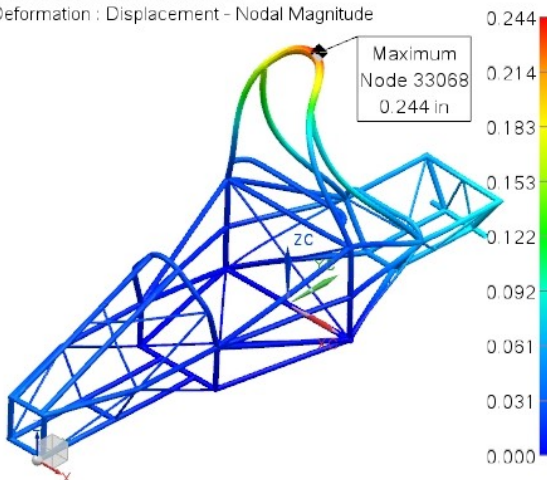


FIGURE 20. Deflection and Von-Mises stress distributions of chassis with 1D elements.

14_sim1 : Main Roll Hoop Result
 Subcase - Static Loads 1, Static Step 1
 Displacement - Nodal, Magnitude
 Min : 0.000, Max : 0.244, Units = in
 Deformation : Displacement - Nodal Magnitude



14_sim1 : Main Roll Hoop Result
 Subcase - Static Loads 1, Static Step 1
 Stress - Element-Nodal, Unaveraged, Von-Mises
 Shell Section : Bending
 Min : 7.51E-014, Max : 6.15E+004, Units = lbf/in²(psi)
 Deformation : Displacement - Nodal Magnitude

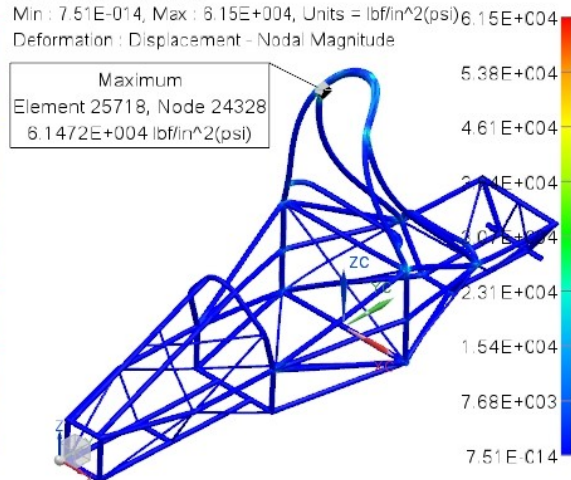


FIGURE 21. Deflection and Von-Mises stress distributions of chassis with 2D elements.

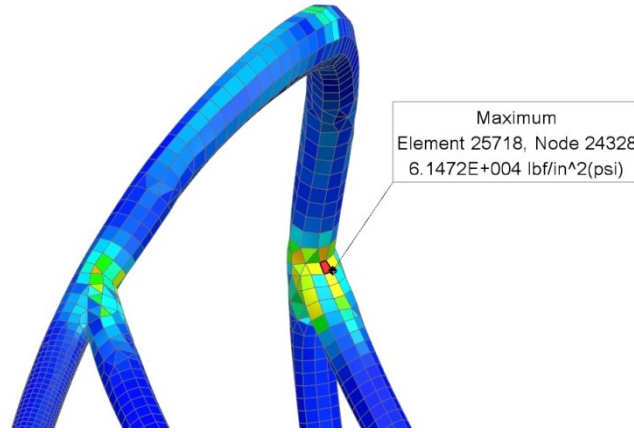


FIGURE 22. Location of maximum stress at joint (shown in red) for 2D element.

3.3. Side Impact Structure

Load applied: $F_x = 7 \text{ kN}$, $F_y = 0 \text{ kN}$, $F_z = 0 \text{ kN}$. Vector direction of lateral load to be in toward the driver. Application point: All structural locations between front roll hoop and main roll hoop in the side impact zone as shown in figure 23. Boundary condition: Fixed displacement (x, y, z) but not rotation of the bottom nodes of both sides of the front and main roll hoops. Max allowable deflection: 1 inch.

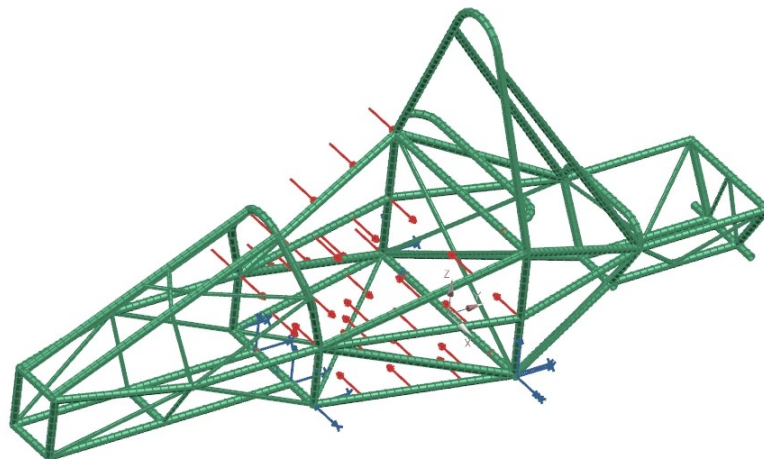


FIGURE 23. FE model for side impact structure simulation.

Results for side impact structure simulation are shown in figure 24 and figure 25. The maximum deformation is 0.09 inches and 0.076 inches for beam and shell elements respectively. The maximum Von-Mises stress is 26016 psi and 59120 psi for beam and shell elements, respectively, which shows relatively higher difference than in previous load cases. However, after a careful examination of 2D elements Von-Mises results, only 14 elements out of 47814 elements had Von-Mises stress greater than 26016 psi and all of them were located at four joints shown in figure 26. This was possibly because of stress concentration at joints. 99.97% of 2D elements had maximum Von-Mises stress less than or equal to 26016 psi.

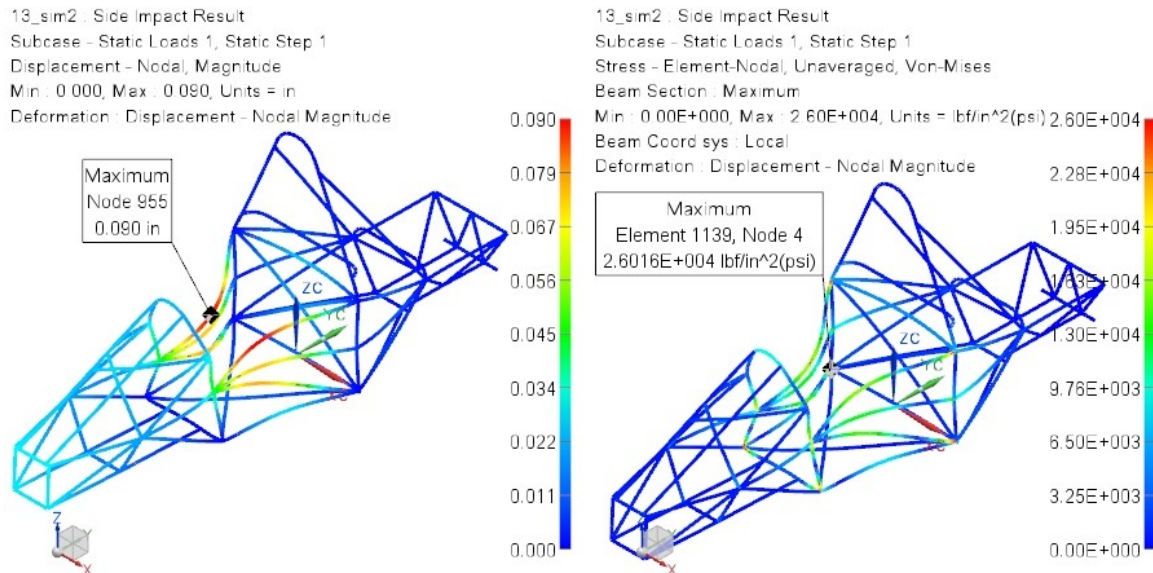


FIGURE 24. Deflection and Von-Mises stress distributions of chassis with 1D elements.

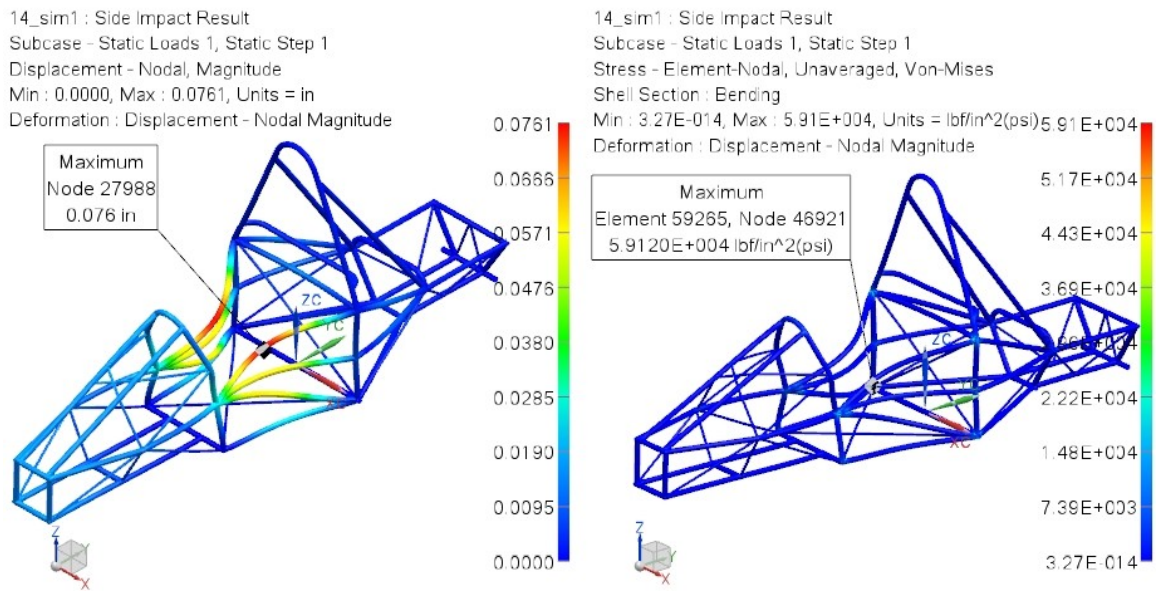


FIGURE 25. Deflection and Von-Mises stress distributions of chassis with 2D elements.

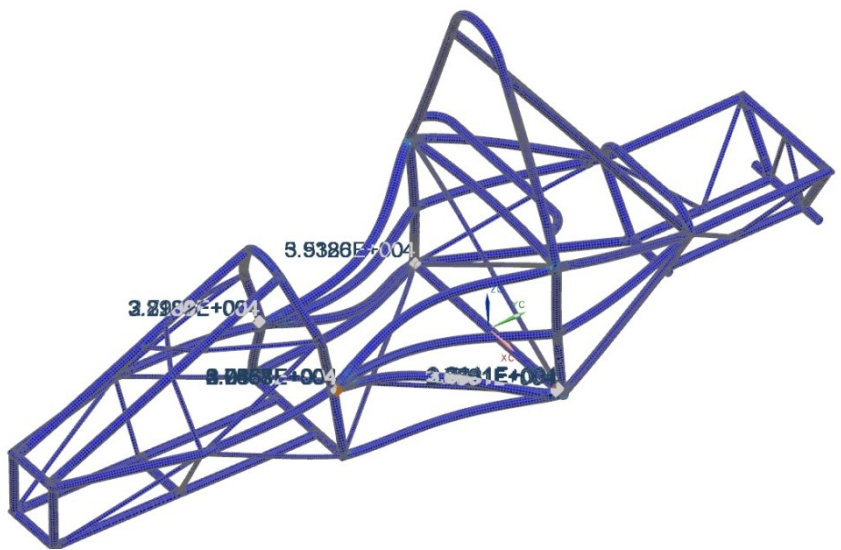


FIGURE 26. Location of four joints with Von-Mises greater than 26016 psi.

3.4. Front Bulkhead & Bulkhead Support

Load applied: $F_x = 0$ kN, $F_y = 150$ kN, $F_z = 0$ kN. Application point:

Attachment points between impact attenuator and front bulkhead as shown in figure 27.

Boundary condition: Fixed displacement (x, y, z) but not rotation of the bottom nodes of both sides of the main roll hoop and both locations where the main hoop and shoulder harness tube connect. Max allowable deflection: 1 inch.

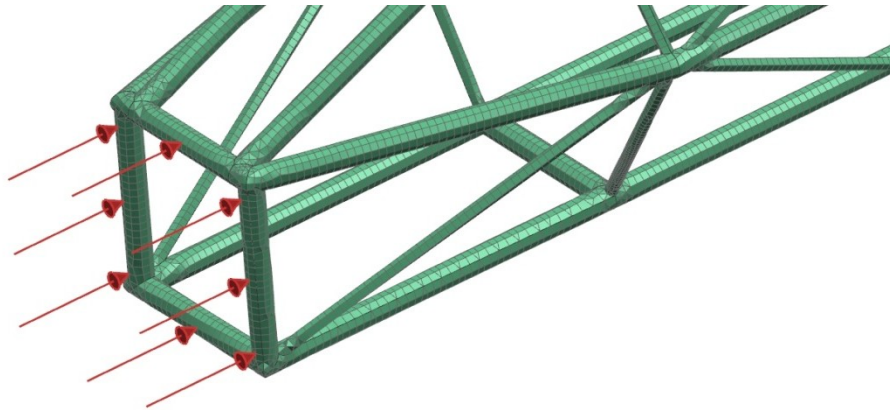


FIGURE 27. Location of load for front bulkhead.

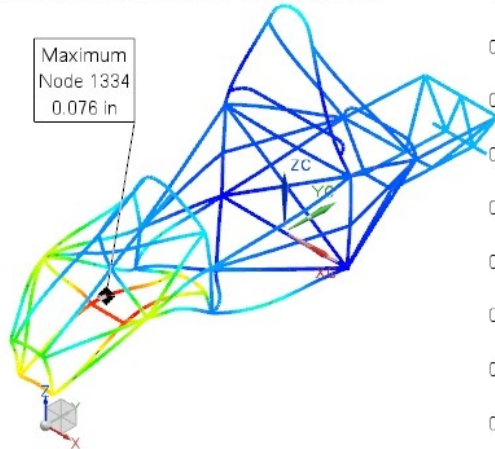
Results are shown in figure 28 and figure 29. The maximum deformation is 0.076 inches and 0.032 inches for beam and shell elements respectively. The maximum Von-Mises stress is 39690 psi and 35540 psi for beam and shell elements respectively.

3.5. Shoulder Harness Attachment

Load applied: 13.2 kN at seat belt attachment angle per attachment point.

Application point: Both harness attachment points simultaneously. Boundary condition: Fixed displacement (x,y,z) but not rotation of the bottom nodes of both sides of the front and main roll hoops. Max Allowable Deflection: 1 inch.

13_sim2 : Front Bulkhead Result
 Subcase - Static Loads 1, Static Step 1
 Displacement - Nodal, Magnitude
 Min : 0.0000, Max : 0.0764, Units = in
 Deformation : Displacement - Nodal Magnitude



13_sim2 : Front Bulkhead Result
 Subcase - Static Loads 1, Static Step 1
 Stress - Element-Nodal, Unaveraged, Von-Mises
 Beam Section : Maximum
 Min : 0.00E+000, Max : 3.97E+004, Units = lbf/in^2(psi)
 Beam Coord sys : Local
 Deformation : Displacement - Nodal Magnitude

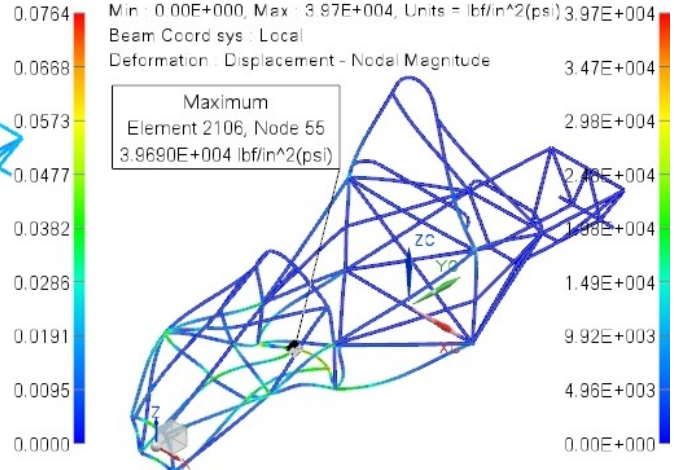
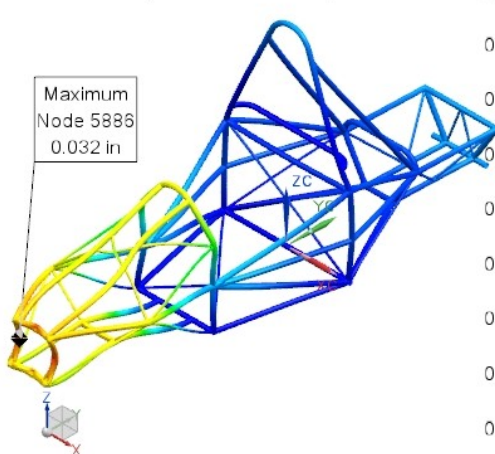


FIGURE 28. Deflection and Von-Mises stress distributions of chassis with 1D elements.

14_sim1 : Front Bulkhead Result
 Subcase - Static Loads 1, Static Step 1
 Displacement - Nodal, Magnitude
 Min : 0.0000, Max : 0.0316, Units = in
 Deformation : Displacement - Nodal Magnitude



14_sim1 : Front Bulkhead Result
 Subcase - Static Loads 1, Static Step 1
 Stress - Element-Nodal, Unaveraged, Von-Mises
 Shell Section : Bending
 Min : 1.15E-015, Max : 3.55E+004, Units = lbf/in^2(psi)
 Deformation : Displacement - Nodal Magnitude

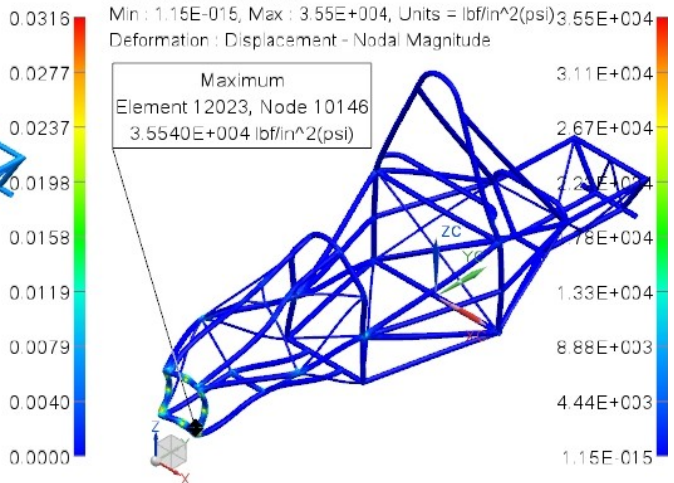


FIGURE 29. Deflection and Von-Mises stress distributions of chassis with 2D elements.

Results are shown in figure 30 and figure 31. The maximum deformation is 0.190 inches and 0.191 inches for beam and shell elements respectively. The maximum Von-Mises stress is 41142 psi and 38392 psi for beam and shell elements respectively which means the shoulder harness attachment was safe as the stress level was below the yield limit of the material.

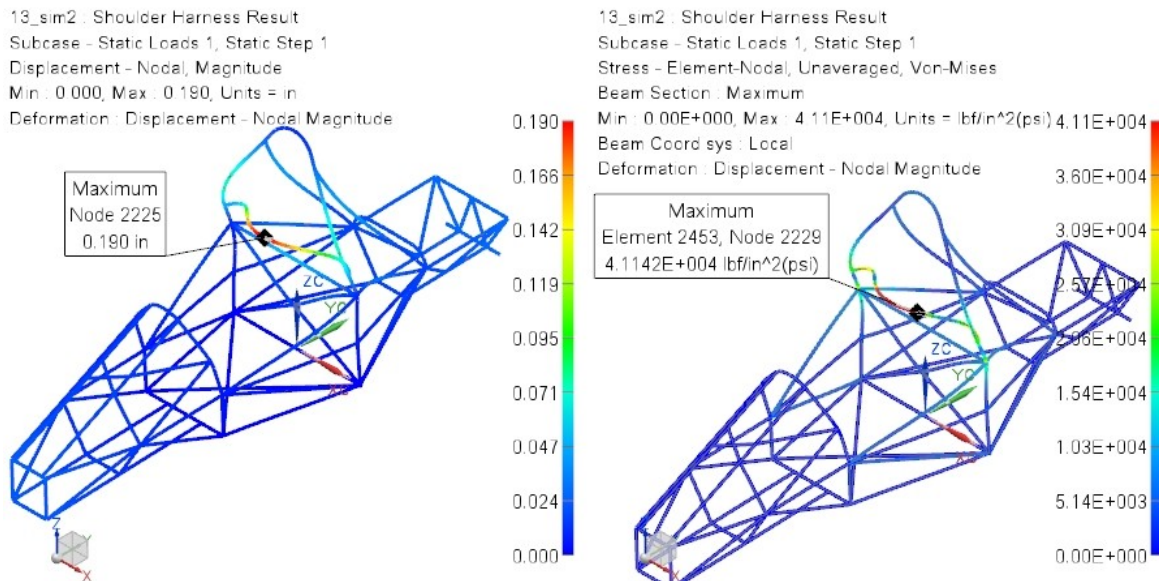


FIGURE 30. Deflection and Von-Mises stress distributions of chassis with 1D elements.

3.6. Torsional Stiffness Test

It is universally recognized that torsional stiffness is one of the most important properties of a vehicle chassis as mentioned in “Race Car Vehicle Dynamics” [6]. When a new racing or sports car is designed, the quality of its chassis is measured by its torsional stiffness. In order to obtain good handling performances, high chassis stiffness, light weight and good weight distribution are some of the important properties of a chassis as described by Costin and Phipps [7].

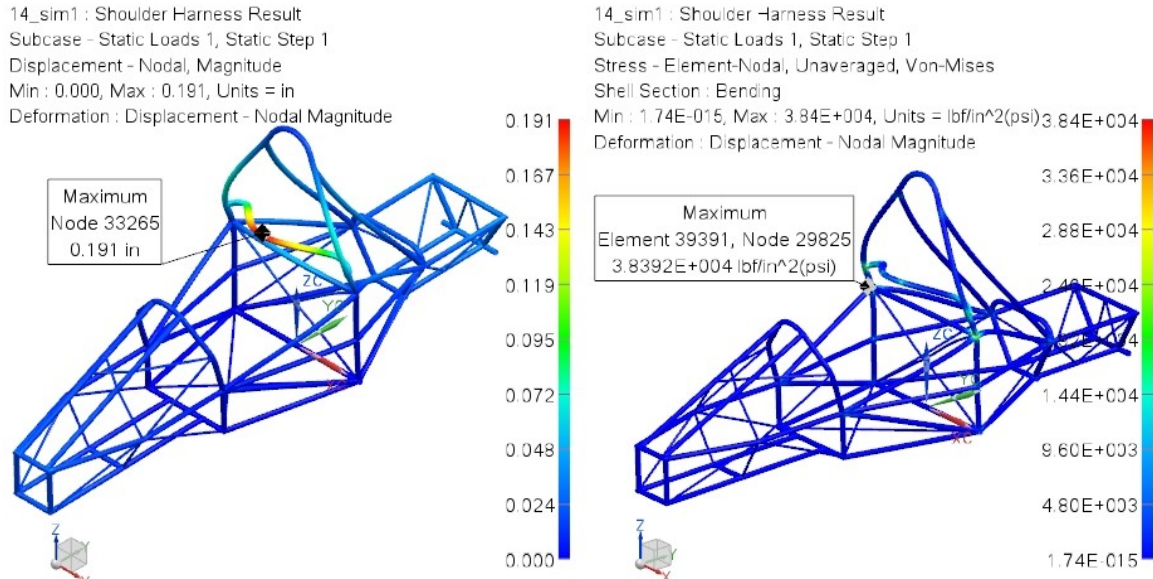


FIGURE 31. Deflection and Von-Mises stress distributions of chassis with 2D elements.

Depending on the shape and manufacture, every structure exhibits a certain resistance to deformation. The term chassis stiffness or rigidity generally indicates resistance to bending while torsional stiffness indicates resistance to twisting. According to Costin and Phipps [7], however, “it is difficult to imagine a chassis that has enough torsional stiffness without having ample rigidity in bending” so that “the criterion of chassis design, and in fact the primary function of a high-performance chassis, is torsional rigidity.” Consequently, this thesis focuses on designing chassis with sufficient torsional stiffness and the term torsional stiffness and stiffness are considered same.

There are several factors that make the torsional rigidity of the chassis an important factor in vehicle dynamics. A chassis with low torsional stiffness has several problems. One of those problems is that the control of lateral load transfer distribution is difficult. Another issue is that displacements of the suspension attachment points increases, so desired control of the movement of tires is not guaranteed. Moreover,

presence of vibrations, resonance and fatigue phenomenon is observed and ultimately, the ride quality is poor.

Torsional rigidity of the frame was calculated using NX simulation. To simulate realistic frame inputs, loads were applied to suspension mount points, rather than the frame forward and rear ends because the ends rarely affected actual driving conditions. Force of 1500 N, 15000 N and 150000 N was applied vertically one by one on front suspension mounting points in opposite direction, downward on left side, upward on right side as shown in figure 32. Fixed constraints were applied on the rear suspension mounting points as shown in figure 33.

Table 2 shows that changing the magnitude of equal and opposite force for creating torque doesn't alter the torsional stiffness. However, changing the location of torsional load changes the value of calculated torsional stiffness. For example, if torsional load was applied on forward upper suspension arms, the calculated torsional stiffness was 1575 Nm/deg, but if the same load was applied on forward lower suspension arms, the calculated torsional stiffness was 602 Nm/deg.

There are four input variables that are used in computing the torsional stiffness. Moment arm length (L), applied load (F), initial moment arm height (h_0), final moment arm height (h_1). The moment arm is the distance measured from the midpoint of chassis to the point of applied load. But in simulation using NX, no h_0 or h_1 are required, because the nodal rotation can directly be taken from the results of simulation. This is the rotation in y direction or the axis parallel to the length of chassis. Results of simulation are shown in figure 34, figure 35, figure 36 and figure 37.

$$\theta = \tan^{-1} \frac{h_o - h_1}{L} \text{ (was taken directly from NX)}$$

$$T = 2.F.L$$

$$K = \frac{T}{\theta}$$

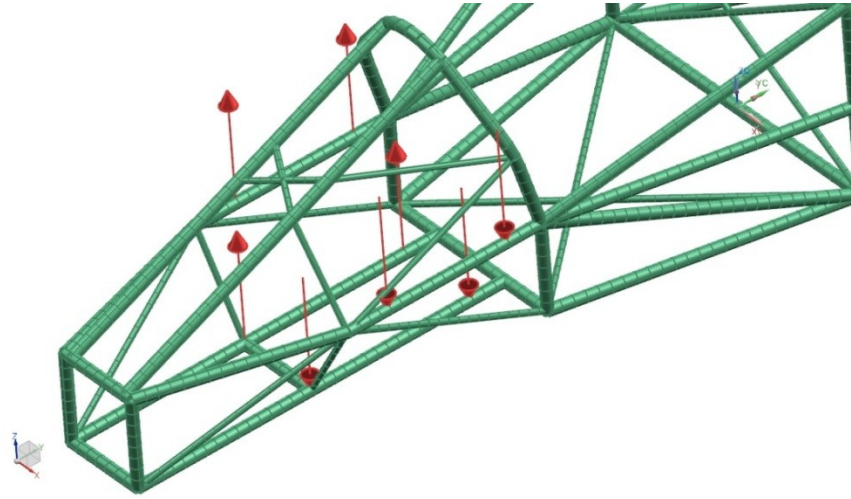


FIGURE 32. Front suspension load application points.

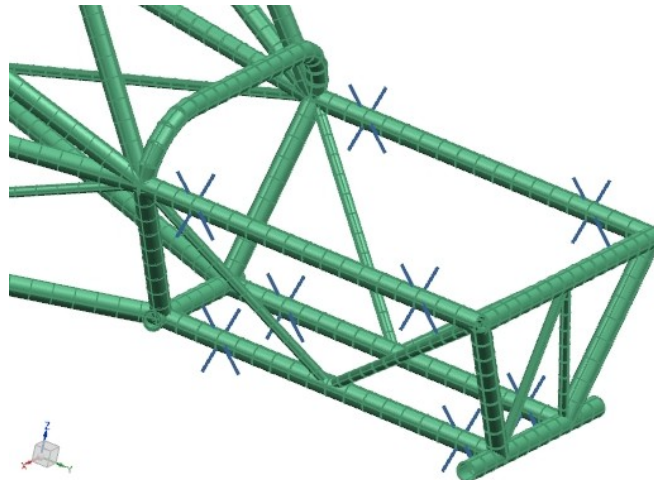


FIGURE 33. Rear suspension fixed constraints.

TABLE 2. Torsional stiffness calculation

Load Case	Load Application Points	Suspension Level	Magnitude of each force F (N)	Torque arm distance L (in)	Torque T (N-m)	Avg. Nodal Rotation on load application points, θ (deg)	Torsional Stiffness, K (N-m/deg)
1	One on forward left, one on forward right	Upper	1500	8	610	0.387	1575
2		Upper	15000	8	6096	3.870	1575
3		Upper	150000	8	60960	38.70	1575
4	One on rear left, one on rear right	Upper	1500	8	610	0.253	2409
5		Upper	15000	8	6096	2.530	2409
6		Upper	150000	8	60960	25.30	2409
7	One on rear left, one on rear right	Lower	1500	4	305	0.169	1804
8		Lower	15000	4	3048	1.690	1804
9		Lower	150000	4	30480	16.90	1804
10	One on forward left, one on forward right	Lower	1500	4	305	0.506	602
11		Lower	15000	4	3048	5.060	602
12		Lower	150000	4	30480	50.60	602

13_sim2 : Torsional Stiffness Result
Case 1, Static Step 1
Rotation - Nodal, Y
Min : -0.018, Max : 0.567, Units = degrees
Deformation : Displacement - Nodal Magnitude

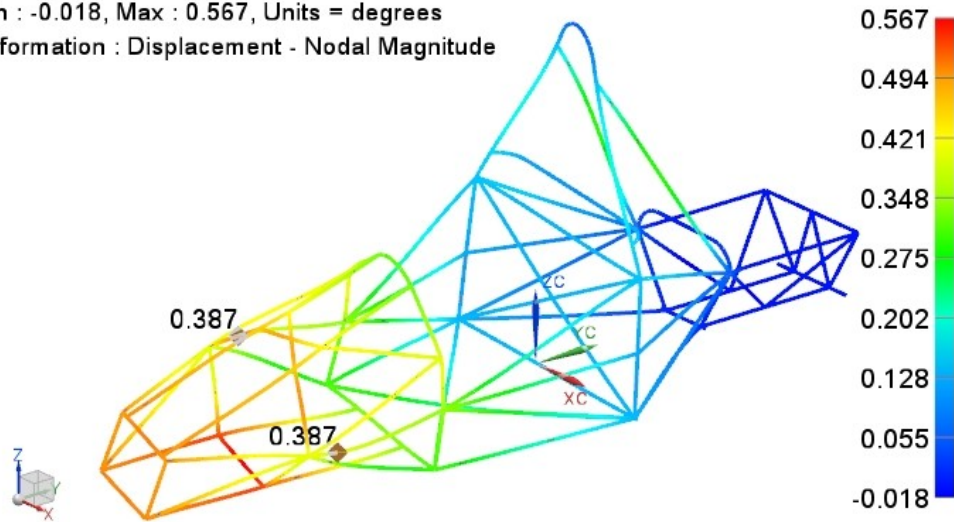


FIGURE 34. Nodal rotation distribution for torsional load case 1.

13_sim2 : Torsional Stiffness Result
Case 4, Static Step 1
Rotation - Nodal, Y
Min : -0.016, Max : 0.419, Units = degrees
Deformation : Displacement - Nodal Magnitude

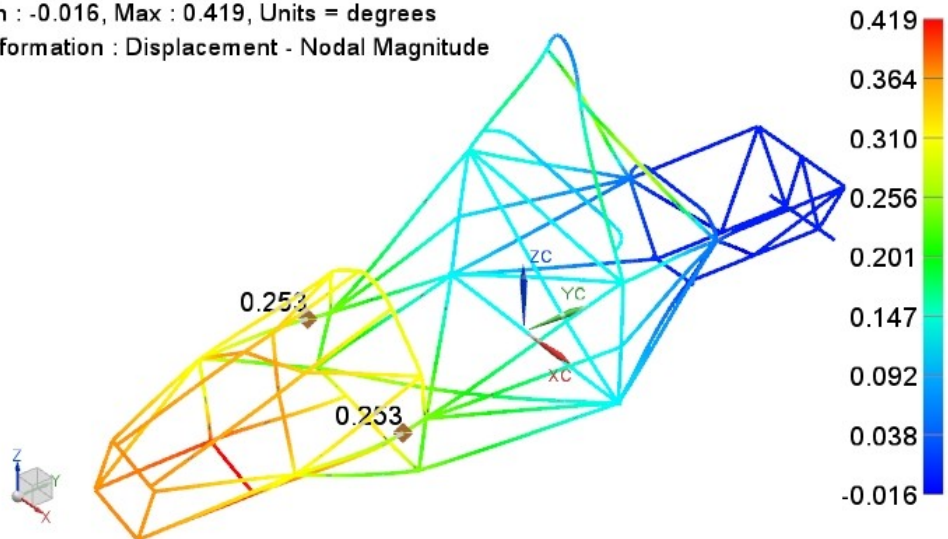


FIGURE 35. Nodal rotation distribution for torsional load case 4.

13_sim2 : Torsional Stiffness Result
Case 7, Static Step 1
Rotation - Nodal, Y
Min : -0.008, Max : 0.244, Units = degrees
Deformation : Displacement - Nodal Magnitude

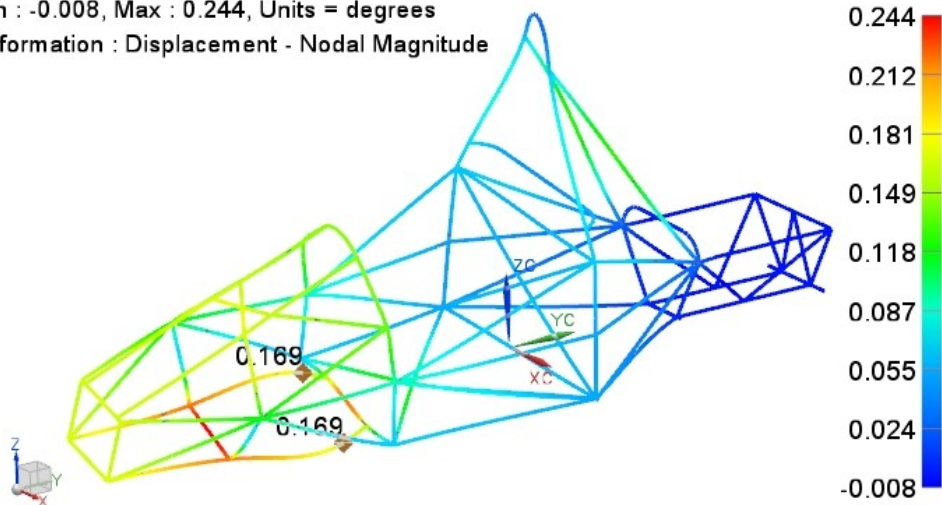


FIGURE 36. Nodal rotation distribution for torsional load case 7.

13_sim2 : Torsional Stiffness Result
Case 10, Static Step 1
Rotation - Nodal, Y
Min : -0.149, Max : 0.597, Units = degrees
Deformation : Displacement - Nodal Magnitude

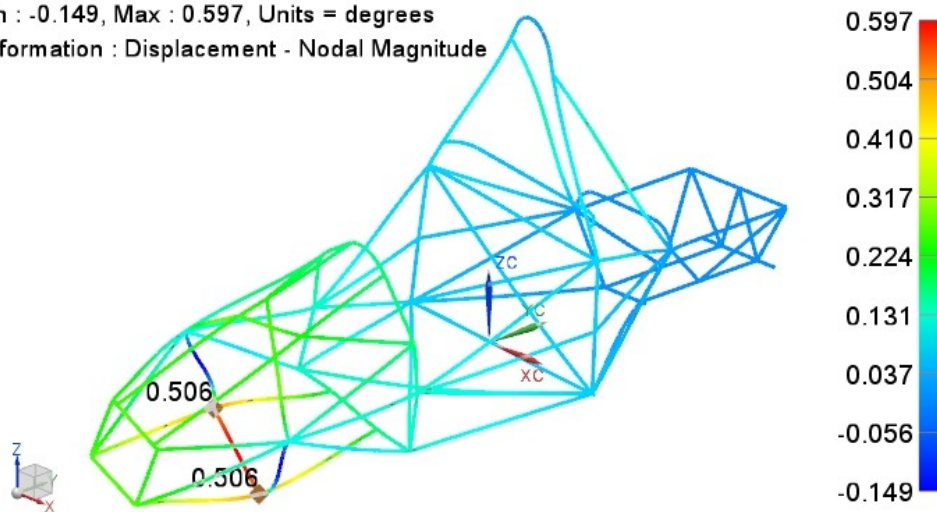


FIGURE 37. Nodal rotation distribution for torsional load case 10.

3.7. Dynamic Analysis

Dynamic response of the system was checked to find out eigen-frequencies and mode shapes. For more realistic representation of the boundary conditions, the suspension arms were also included along with the chassis model. Simply supported constraints were applied on the front suspension arms at the location where they were supposed to be rested on the wheel as shown in figure 38. Simply supported here means that all of the translations are fixed and all rotations are free except rotation in z-direction which is fixed. Fixed constraints were applied at the rear suspension arms at the location where they were meant to be supported on the wheel as shown in figure 39. In NX-8, solution type SEMODES 103 was selected which doesn't require loads to be specified for the analysis. First five mode shapes of the frame were observed at frequencies 34 Hz, 36 Hz, 57 Hz, 73 Hz and 102 Hz. The deformed shapes are shown in figure 40, figure 41 and figure 42.

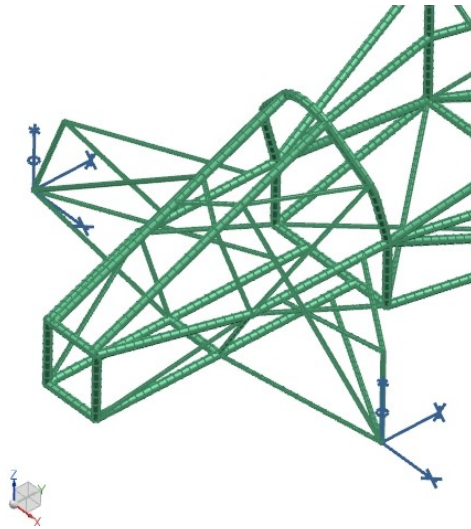


FIGURE 38. FE model showing simply supported constraints at front suspension.

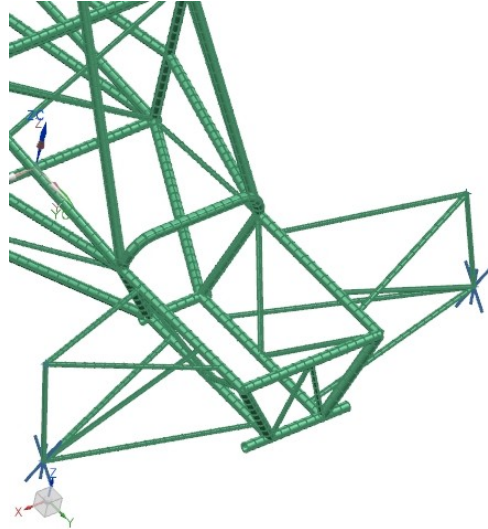


FIGURE 39. FE model showing fixed constraints at rear suspension.

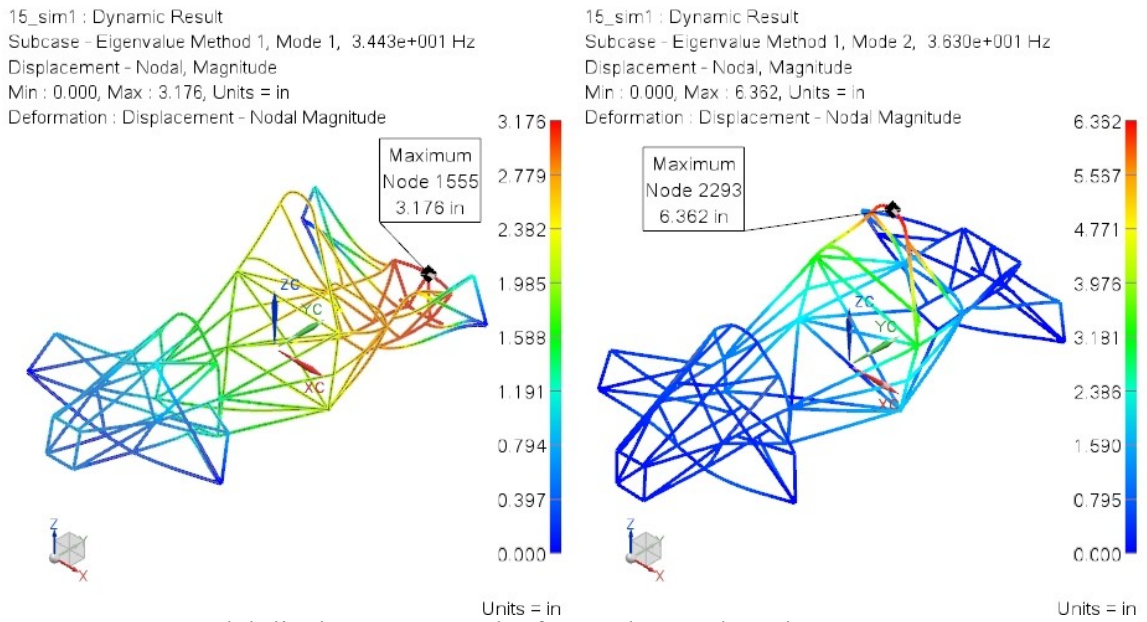


FIGURE 40. Nodal displacement results for mode 1 and mode 2.

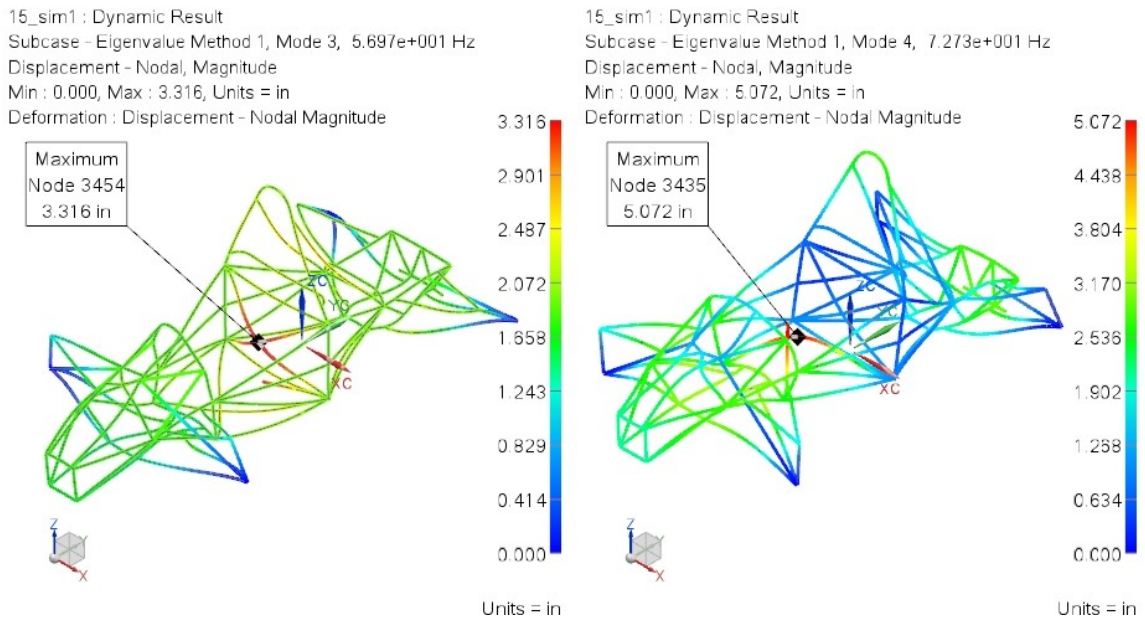


FIGURE 41. Nodal displacement results for mode 3 and mode 4.

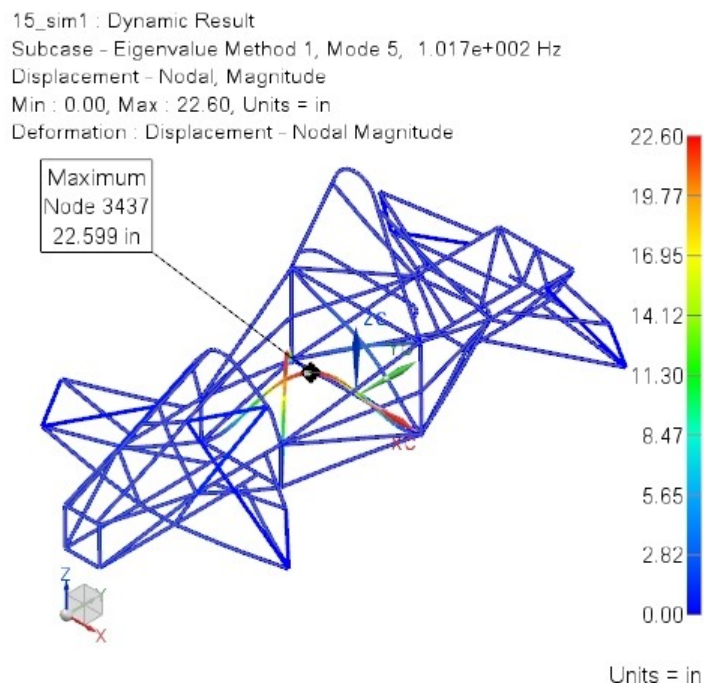


FIGURE 42. Nodal displacement results for mode 5.

The blue color in the figure represents regions with minimum deformations whereas the red color represent regions with maximum deformation. It can be observed that for the first four modes, deformation is distributed on the overall frame. The fifth mode shape shows the deformation of two cross-bracings on the bottom of cockpit only and relatively low or no deformation at all for the rest of the frame. This shows that these bracings are more sensitive to dynamic load than the rest of the frame. Either thicker tubes may be used to fabricate those bracings or some gusset plates may be provided to protect these bracings to undergo huge deformations. For this study, the second option was selected, so that for optimization, the initial thickness of these bracings remain the same as the other tube members of same category described in section 1.3.1.

All five eigenvectors show that the space of the driver is not reduced during dynamic deformation. But it is recommended for future constructions to increase the thickness of the main roll hoop and front roll hoop.

CHAPTER 4

OPTIMIZATION

The main purpose of chassis optimization was to reduce weight without sacrificing strength requirements. This was done in two different ways. First option was K/W method (torsional stiffness to weight ratio) and the second was geometry optimization using NX-8.

4.1. K/W Method

In this method, ratio of torsional stiffness to chassis weight was used as the basis for optimization. The candidate solution with a high K/W ratio was considered to be optimal. Different thickness sets for primary, secondary and tertiary tube members were created and named as Thickness Set 1, Thickness Set 2, , Thickness Set 7. Static analysis was done with NX as described in sections 3.1 to 3.5 (five simulations). Maximum displacement and Von-Mises stress values for each simulation and each thickness set were obtained by changing physical properties of PBEAM element in NX and were tabulated in table 3 and table 4. For five simulation types and seven thickness sets, this step took 35 NX simulation runs to get results for each candidate solution.

After careful examination of displacement and Von-Mises stress values given in table 3 and table 4, it was concluded that the chassis was safe under all loading conditions except the front roll hoop. The simulation results for front roll hoop show Von-Mises stresses to be higher than yield strength of AISI-4130 steel; 66717 psi, except for the

third thickness-set whose maximum Von-Mises stress is below yield limit. However, this thickness-set generates a weight of 98.89 lb which is high, and the objective of optimization was to minimize weight. Therefore, the conclusion was to provide some gussets on both left and right sides of front roll hoop in order to prevent failure under the described loading conditions.

TABLE 3. Displacement results for simulations with different tube thicknesses

Thickness Set		1	2	3	4	5	6	7
Thickness	Primary (in)	0.095	0.120	0.156	0.120	0.120	0.120	0.120
	Secondary (in)	0.065	0.065	0.065	0.083	0.095	0.065	0.065
	Tertiary (in)	0.065	0.065	0.065	0.065	0.065	0.049	0.058
Front Roll Hoop	Disp. (in)	0.358	0.315	0.278	0.305	0.299	0.317	0.316
Main Roll Hoop	Disp. (in)	0.272	0.249	0.230	0.228	0.219	0.253	0.251
Side Impact	Disp. (in)	0.097	0.090	0.083	0.082	0.078	0.090	0.090
Front Bulkhead	Disp. (in)	0.083	0.076	0.070	0.071	0.068	0.077	0.077
Shoulder Harness	Disp. (in)	0.218	0.190	0.166	0.185	0.183	0.190	0.190
Weight	(lb)	79.93	88.07	98.89	96.46	101.85	85.67	87.05

TABLE 4. Von-Mises stress results for simulations with different tube thicknesses

Thickness Set		1	2	3	4	5	6	7
Front Roll Hoop	Stress (psi)	82600	71572	62100	70400	69700	71900	71700
Main Roll Hoop	Stress (psi)	64700	54872	46800	55100	55200	54500	54700
Side Impact	Stress (psi)	28300	26016	25700	24100	24000	26000	26000
Front Bulkhead	Stress (psi)	45300	39690	34800	39400	39300	40600	40000
Shoulder Harness	Stress (psi)	48100	41142	35300	40900	40800	41200	41158

Similarly, torsional stiffness simulations were also performed for seven thickness categories and for four load cases 1, 4, 7 and 10. The other load cases were eliminated because they didn't affect torsional stiffness. So, this step took 28 NX simulations to provide results for each candidate solution. The score was determined by dividing weight of each candidate solution with its torsional stiffness as per Auer's work [8].

$$Score = \frac{K}{W}$$

where,

K = Torsional Stiffness (N-m/deg).

W = Weight of the chassis (lb).

All of the scores for these four load cases were added to find out total score for each thickness category as shown in table 5. Based on that, it was determined that thickness set 1 is the best solution with the highest score of 75, which means it offers high torsional stiffness with low weight as compared to others. This consisted with 0.095, 0.065 and 0.065 inches wall thickness tubes for primary, secondary and tertiary members that make overall weight of the chassis to be 79.93 lb.

4.2. Geometry Optimization Via NX-8

This method was much easier and quicker than the one described above and took just three NX optimization runs as compared to 63 (35 + 28) simulations in the previous method. It used Altair HyperOpt tool for design optimization present in NX-8. This consists of defining objective function, constraints, design variables and some other information such as number of iterations.

TABLE 5. Nodal rotation and torsional stiffness values

Thickness Set		1	2	3	4	5	6	7
Load Case 1	θ (deg)	0.42	0.39	0.36	0.35	0.33	0.39	0.39
	K (Nm/deg)	1465	1575	1689	1747	1847	1567	1571
	Score (K/W)	18	18	17	18	18	18	18
Load Case 4	θ (deg)	0.27	0.25	0.24	0.23	0.22	0.26	0.25
	K (Nm/deg)	2258	2409	2572	2685	2835	2381	2400
	Score (K/W)	28	27	26	28	28	28	28
Load Case 7	θ (deg)	0.18	0.17	0.16	0.16	0.15	0.17	0.17
	K (Nm/deg)	1675	1804	1929	1966	2059	1762	1782
	Score (K/W)	21	20	20	20	20	21	20
Load Case 10	θ (deg)	0.52	0.51	0.49	0.46	0.43	0.54	0.52
	K (Nm/deg)	583	602	621	666	702	570	590
	Score (K/W)	7	7	6	7	7	7	7
Total	Total Score	75	73	69	73	73	73	73

The optimization problem was formulated as follows:

Design Objective:

Minimize Model Weight

Design Constraints:

Model Von-Mises Stress, Upper limit = 66717 lbf/in²(psi)

Design Variables:

TUBE(1)(ri), Initial value = 0.380, Lower limit = 0.344, Upper limit = 0.405

TUBE(2)(ri), Initial value = 0.435, Lower limit = 0.405, Upper limit = 0.435

TUBE(3)(ri), Initial value = 0.185, Lower limit = 0.185, Upper limit = 0.201

TUBE(4)(ri), Initial value = 0.380, Lower limit = 0.344, Upper limit = 0.405

Maximum Number of Iterations: 20

Convergence Parameters:

Max Constraint Violation (%): 2.500000

Relative Convergence (%): 2.500000

Absolute Convergence: 0.001000

Perturbation Fraction: 0.200000

where,

TUBE(1)(ri) = Internal radius of primary tube members except front roll hoop.

TUBE(2)(ri) = Internal radius of secondary tube members.

TUBE(3)(ri) = Internal radius of tertiary tube members.

TUBE(4)(ri) = Internal radius of front roll hoop tube members.

Model weight minimization was defined as the objective. Maximum Von-Mises stress was set to be 66717 psi as design constraint. This value was the yield strength of material and it was used so that for every successful solution, the maximum stress induced in the structure doesn't exceed the yield limit. For design variable, only the minimum and maximum limits for the tube internal radii were provided in the properties of beam section. This was the key step for saving time for optimization as the previous optimization procedure required each individual thickness to be analyzed separately. With geometry optimization, only range was defined for thickness and NX increased or decreased this value automatically as required for reducing weight while maintaining Von-Mises stress below yield limit. Fourth category of tube for front roll hoop was especially created because simulation for front roll hoop showed Von-Mises stresses

higher than yield limit. In fact, design variables for each individual tube could be created for sensitivity analysis, if required, to find out how much each tube contributes to increase the total frame weight and Von-Mises stress.

This optimization was done in three steps.

4.2.1. Step 1

First optimization was for main roll hoop, side impact and shoulder harness attachment simulations. All of these simulations share same set of boundary conditions, so all of them were merged under one solution with different load-cases and one optimization process was enough for these three simulations.

The optimization results are given in table 6 which shows that fifth iteration or design cycle offers the most optimized design with total chassis weight of 77.55 lb. This consisted of tubes with internal radii of 0.405, 0.435, 0.201 and 0.405 inches. This means wall thicknesses of 0.095, 0.065, 0.049 and 0.095 inches for primary, secondary, tertiary and front roll hoop tube members. Charts for design objective and design constraints were also produced as the result of optimization run to provide user with a graphical representation of the iterations. These graphs are shown in figure 43, figure 44, figure 45, figure 46 and figure 47.

TABLE 6. Optimization via NX, step 1

Optimization History based on Altair HyperOpt						
Iteration (Design Cycle)	0	1	2	3	4	5
Design Objective Function Results						
Minimum Weight [lb]	88.11	84.65	90.94	87.64	87.65	77.55
Design Variable Results (tube internal diameter in inches)						
TUBE(1)(DIM2)	0.380	0.392	0.380	0.380	0.380	0.405
TUBE(2)(DIM2)	0.435	0.435	0.429	0.435	0.435	0.435
TUBE(3)(DIM2)	0.185	0.185	0.185	0.188	0.185	0.201
TUBE(4)(DIM2)	0.380	0.380	0.380	0.380	0.392	0.405
Design Constraint Results						
Von-Mises [psi]	54872	59048	54962	54802	54871	64237
No better design could be found, run converged.						

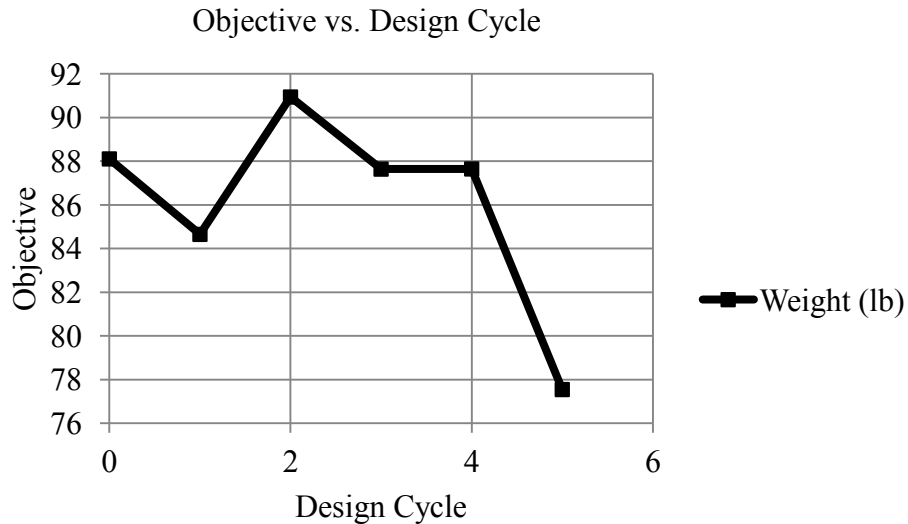


FIGURE 43. Objective function graph for step 1.

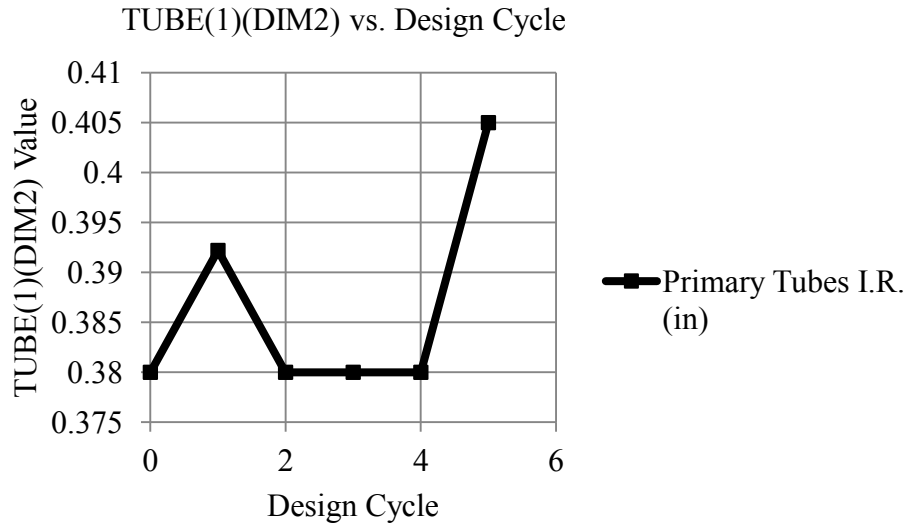


FIGURE 44. First constraint graph for optimization step 1.

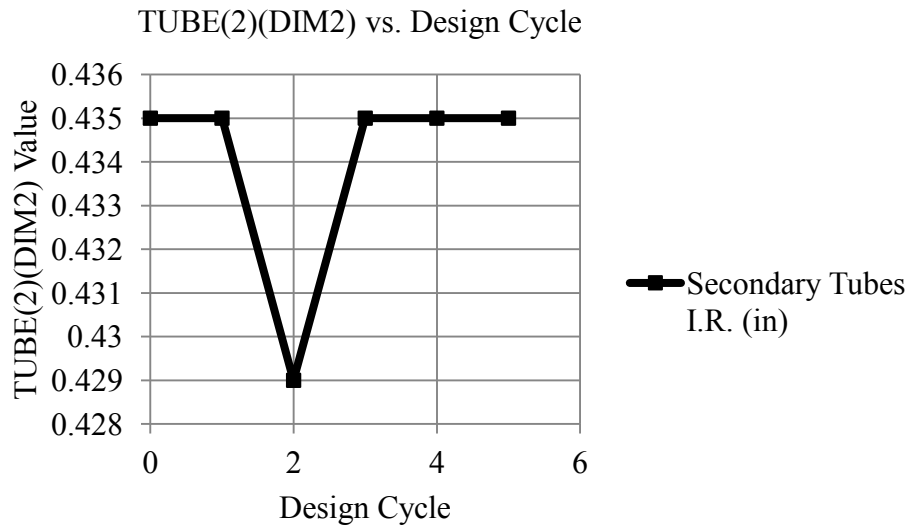


FIGURE 45. Second constraint graph for optimization step 1.

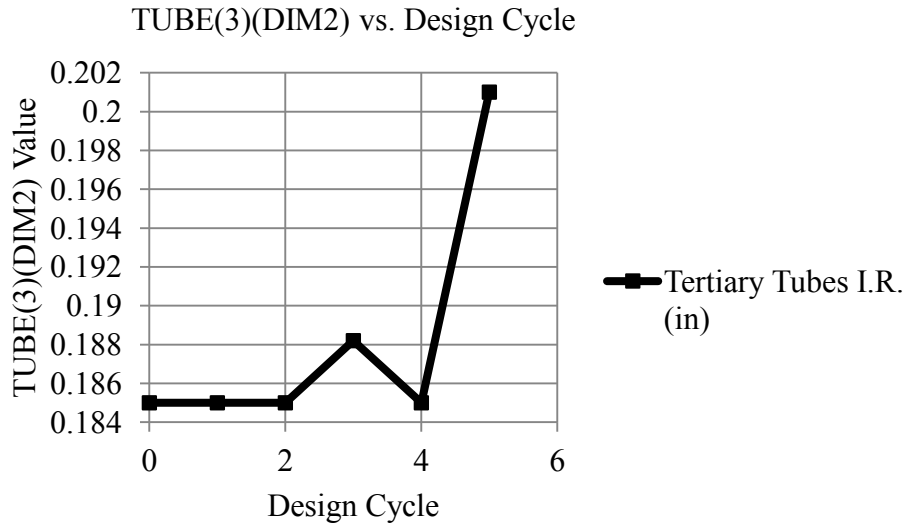


FIGURE 46. Third constraint graph for optimization step 1.

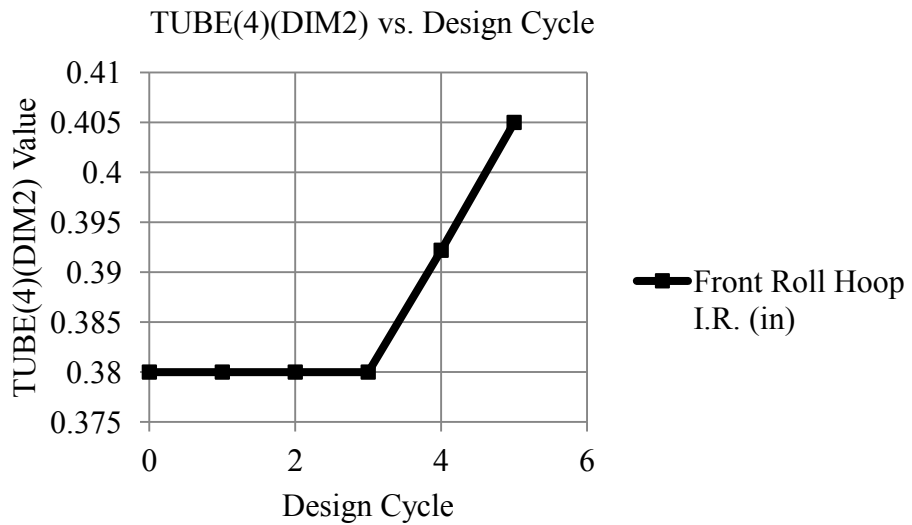


FIGURE 47. Fourth constraint graph for optimization step 1.

4.2.2. Step 2

Second optimization was done for front bulkhead simulation. This simulation could not be merged under the other simulations because it has different boundary conditions. . The optimization results are given in table 7 which shows that optimization run converged on fifth design cycle with the same chassis weight of 77.44 lb and with the same internal radii; 0.405, 0.435, 0.201 and 0.405 as was obtained in previous optimization step. Graphs for design objective and design constraints for this step are shown in figure 48, figure 49, figure 50, figure 51 and figure 52.

TABLE 7. Optimization via NX, step 2

Optimization History based on Altair HyperOpt						
Iteration (Design Cycle)	0	1	2	3	4	5
Design Objective Function Results						
Minimum Weight [lb]	88.10	84.65	90.94	87.64	87.65	77.55
Design Variable Results (tube internal diameter in inches)						
TUBE(1)(DIM2)	0.380	0.392	0.380	0.380	0.380	0.405
TUBE(2)(DIM2)	0.435	0.435	0.429	0.435	0.435	0.435
TUBE(3)(DIM2)	0.185	0.185	0.185	0.188	0.185	0.201
TUBE(4)(DIM2)	0.380	0.380	0.380	0.380	0.392	0.405
Design Constraint Results						
Von-Mises [psi]	39690	41911	39599	39842	39868	46395
No better design could be found, run converged.						

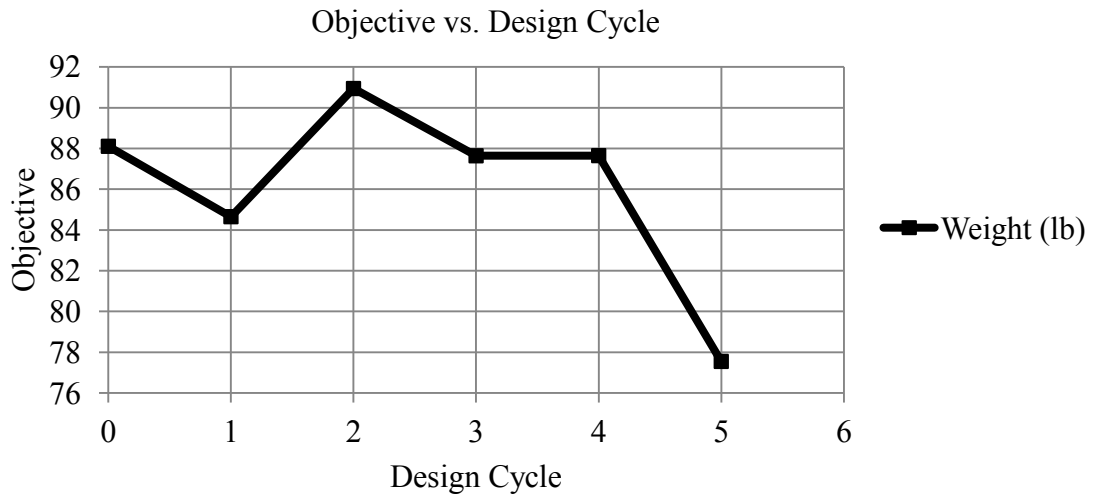


FIGURE 48. Objective function graph for optimization step 2.

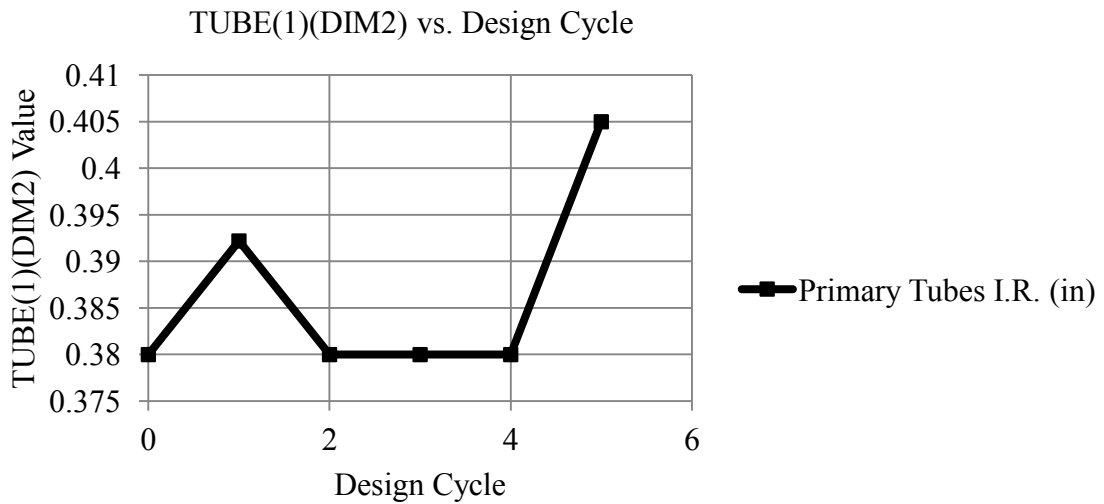


FIGURE 49. First constraint graph for optimization step 2.

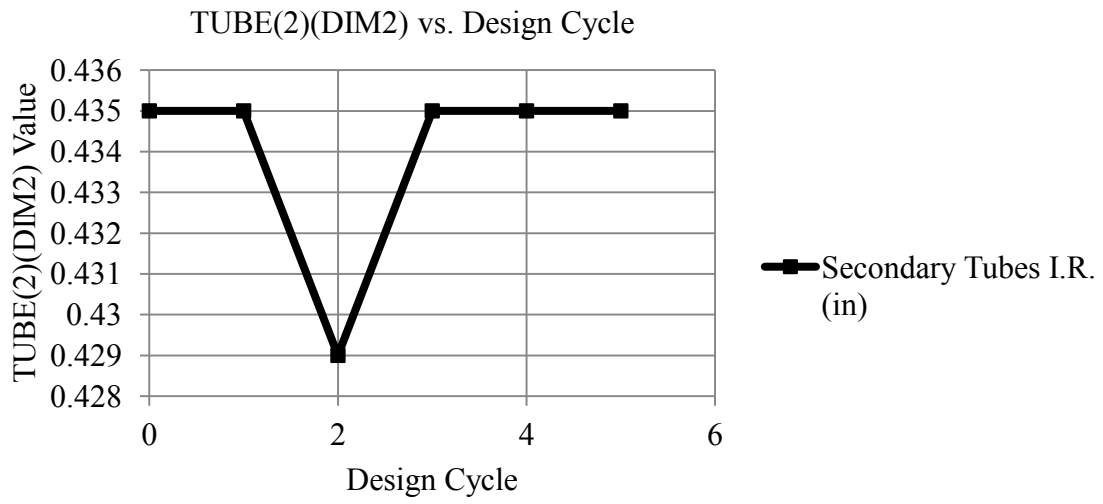


FIGURE 50. Second constraint graph for optimization step 2.

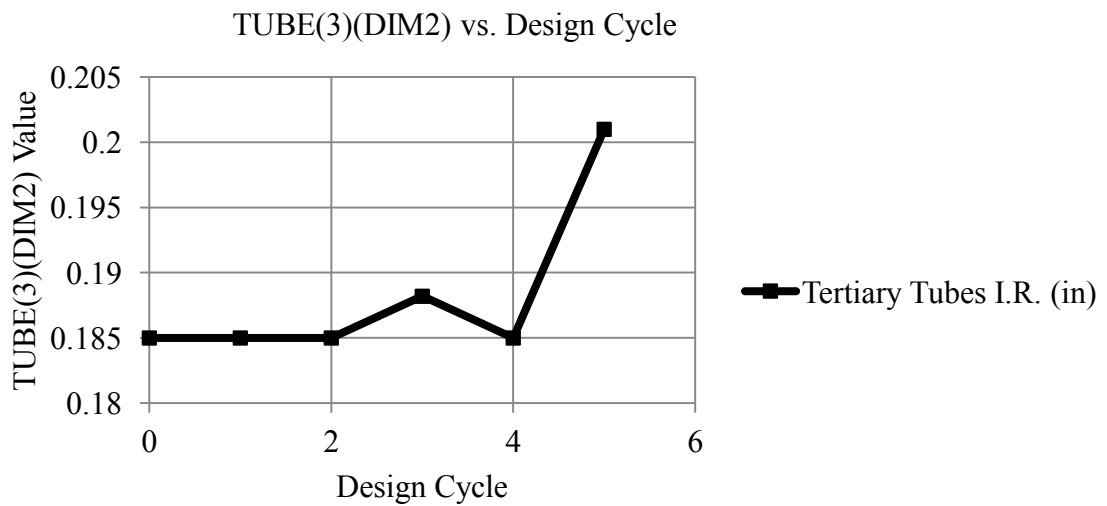


FIGURE 51. Third constraint graph for optimization step 2.

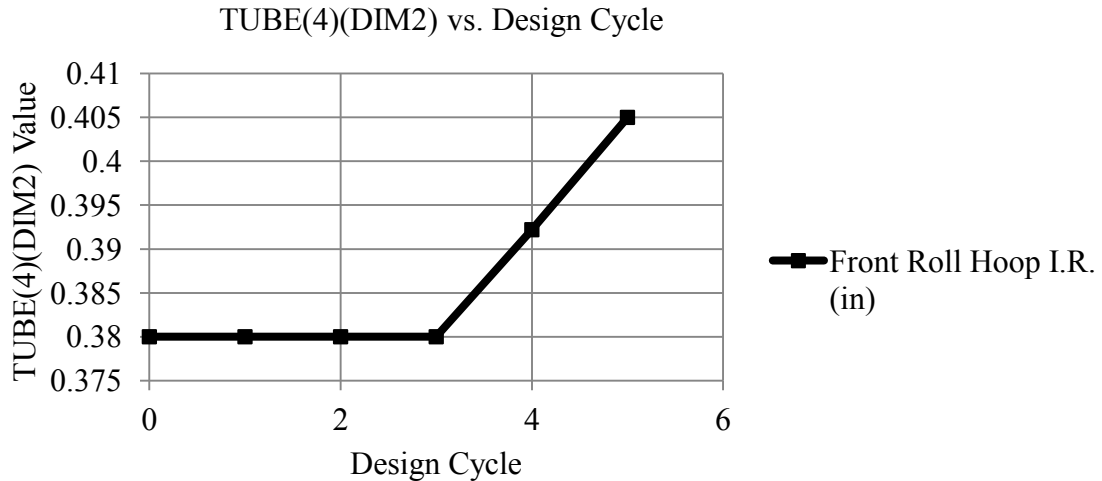


FIGURE 52. Fourth constraint graph for optimization step 2.

4.2.3. Step 3

Third optimization was done for front roll hoop simulation. Although it shares same boundary conditions as main roll hoop, side impact and shoulder harness simulations, it was done separately because front roll hoop results showed Von-Mises stress higher than yield limit in section 3.1. So, fourth category of tubes was created especially for front roll hoop. If an increase in thickness is required for front roll hoop, it doesn't increase the thickness of other primary tube members. The optimization results are given in table 8 which shows eighteenth iteration offers the most optimized design with total chassis weight of 80.76 lb. This consisted of tubes with internal radii of 0.402, 0.435, 0.201 and 0.344 inches or wall thicknesses of 0.098, 0.065, 0.049 and 0.156 inches for primary, secondary, tertiary and front roll hoop tube members. Since tube with wall thickness of 0.098 is not commercially available, the next higher thickness 0.12 inches could be selected for primary tube members. Graphs for design objective and design constraints are shown in figure 53, figure 54, figure 55, figure 56 and figure 57.

TABLE 8. Optimization via NX, step 3

Optimization History based on Altair HyperOpt						
Iteration (Design Cycle)	0	1	8	9	17	18
Design Objective Function Results						
Minimum Weight [lb]	88.10	84.65	79.75	83.72	80.76	80.76
Design Variable Results (tube internal diameter in inches)						
TUBE(1)(DIM2)	0.380	0.392	0.405	0.391	0.402	0.402
TUBE(2)(DIM2)	0.435	0.435	0.430	0.435	0.435	0.435
TUBE(3)(DIM2)	0.185	0.185	0.201	0.201	0.201	0.201
TUBE(4)(DIM2)	0.380	0.380	0.405	0.344	0.344	0.344
Design Constraint Results						
Von-Mises [psi]	71572	71914	82638	63305	66718	66712
Small change in design, run converged.						

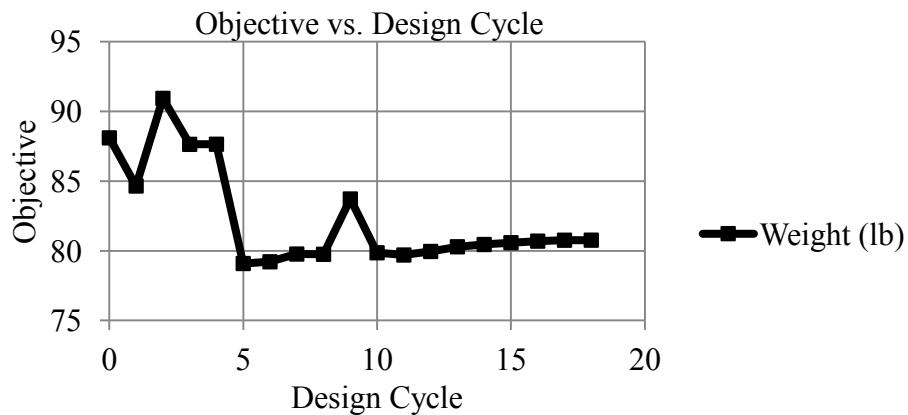


FIGURE 53. Objective function graph for optimization step 3.

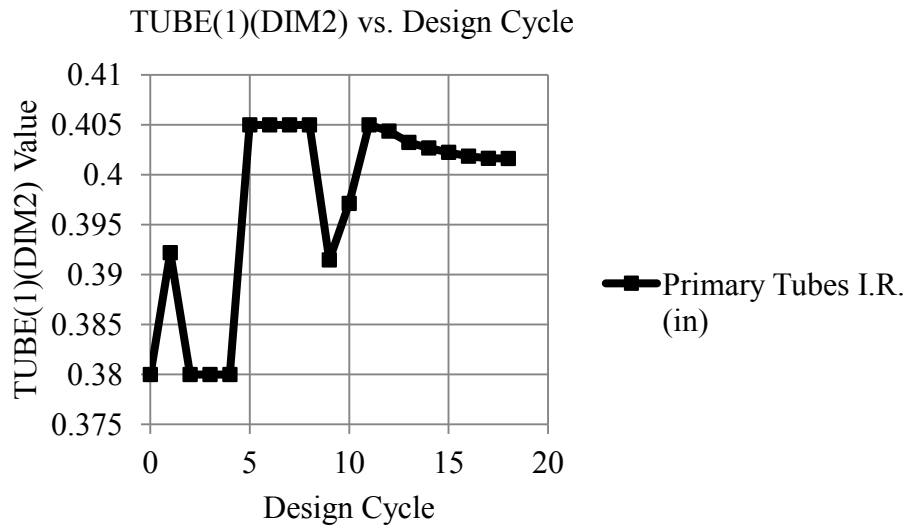


FIGURE 54. First constraint graph for optimization step 3.

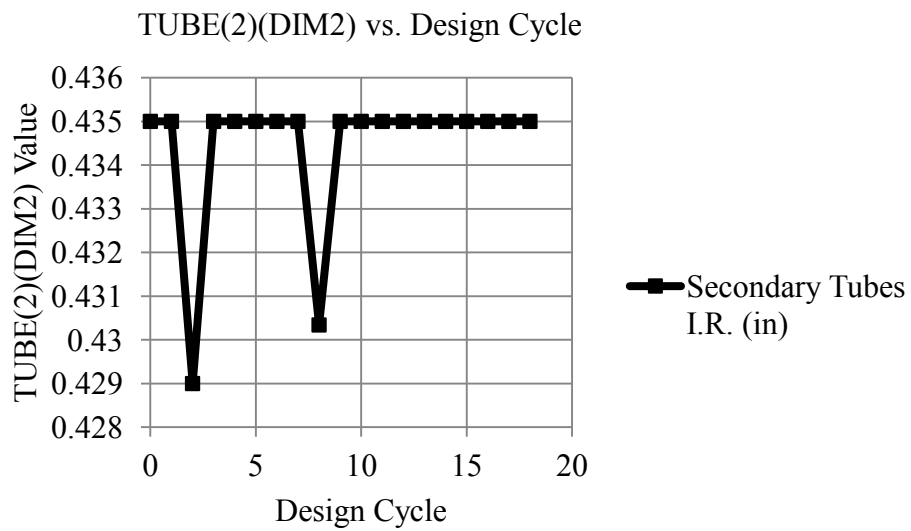


FIGURE 55. Second constraint graph for optimization step 3.

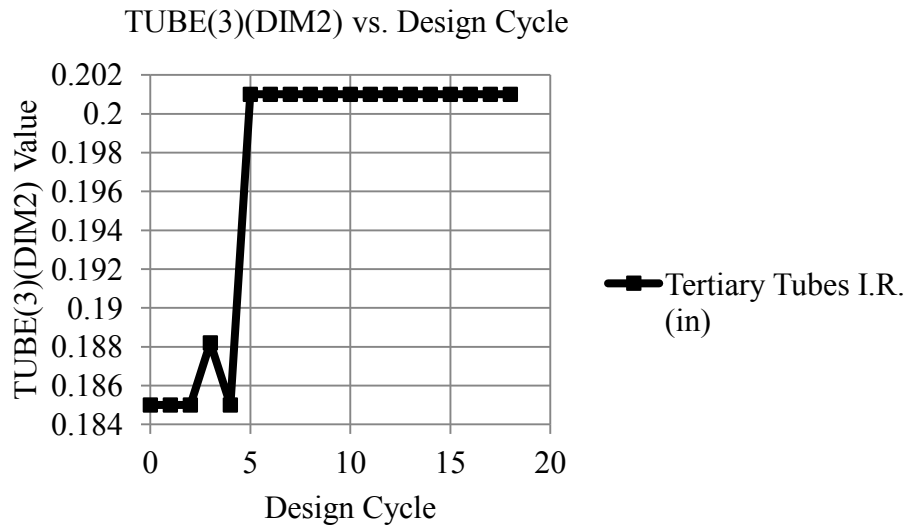


FIGURE 56. Third constraint graph for optimization step 3.

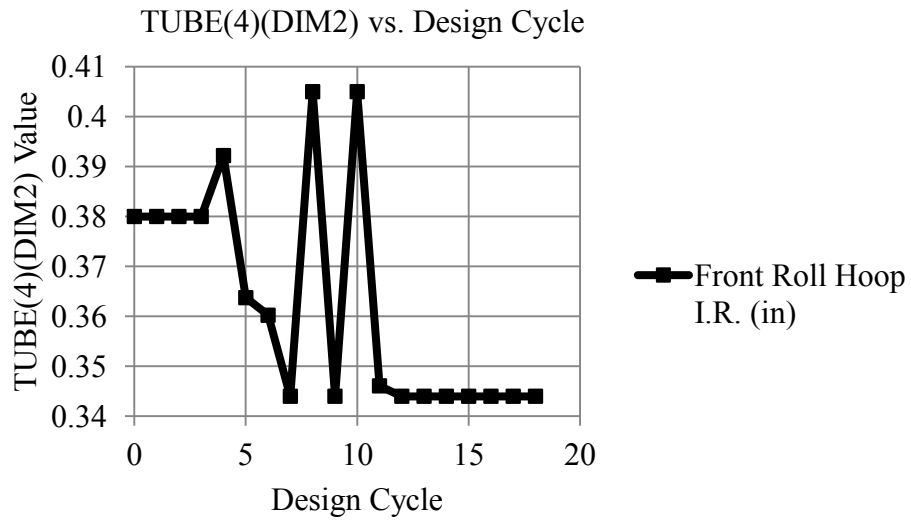


FIGURE 57. Fourth constraint graph for optimization step 3.

4.3. Final Observation

The optimization procedure in NX is based on the Quasi Newton Method. It is the fastest numerical procedure for all nonlinear problems in engineering. The objective can be the constraint minimizing of the weight. The same procedure can be applied for buckling, eigenvector and shape design. Shape design can be used to select elements.

CHAPTER 5

FINAL DESIGN

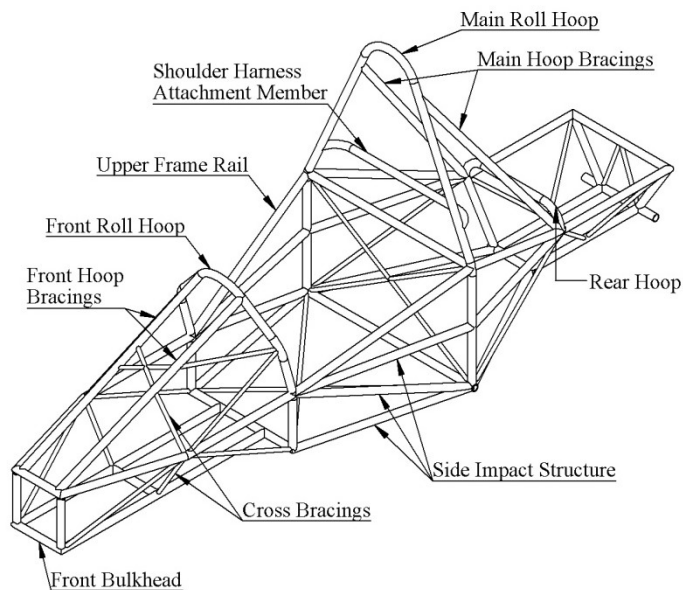


FIGURE 58. Final design

Based on optimization results in previous chapter, the final design consisted of 0.12 inch thick primary tube members except front roll hoop, 0.065 inch thick secondary tube members, 0.049 inch thick tertiary members and 0.156 inch thick front roll hoop. The final design with names of tube members is shown in figure 58.

The main concept behind 2012 chassis was to build it tight and compact. The basic design features of the chassis taken from the previous chassis design were

developed to increase strength and stiffness and to comply with the updated competition rules for 2012. These features include wheelbase, track width, overall dimensions of the frame, main roll hoop and front roll hoop location. These dimensions are shown in figure 59 and figure 60.

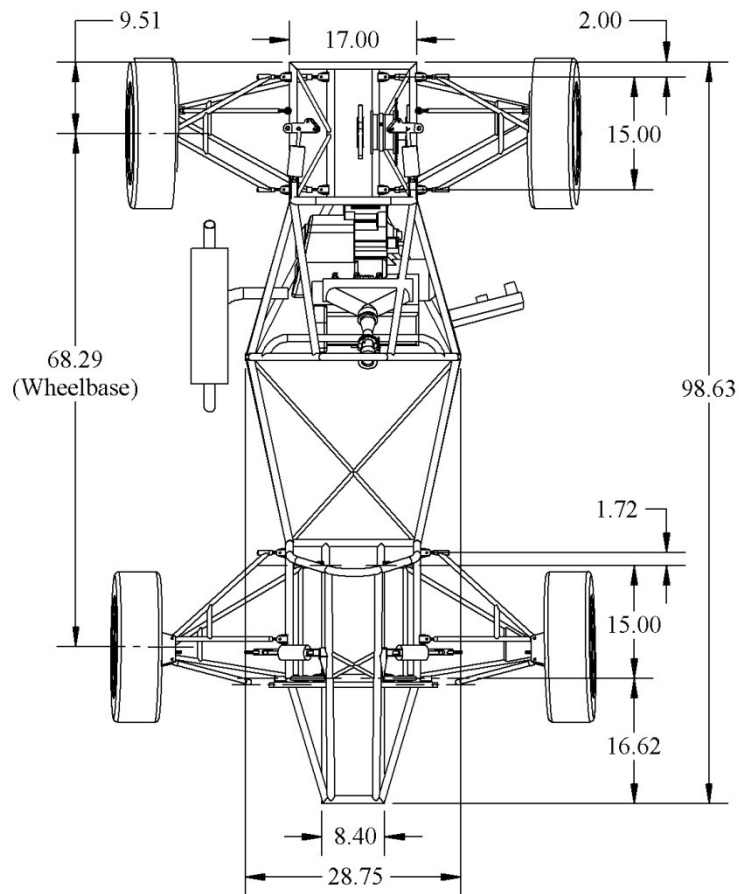


FIGURE 59. 2012 CSULB FSAE showing general dimensions (top view).

The frame can be divided into three compartments; front cradle, cockpit and rear cradle as shown in table 9.

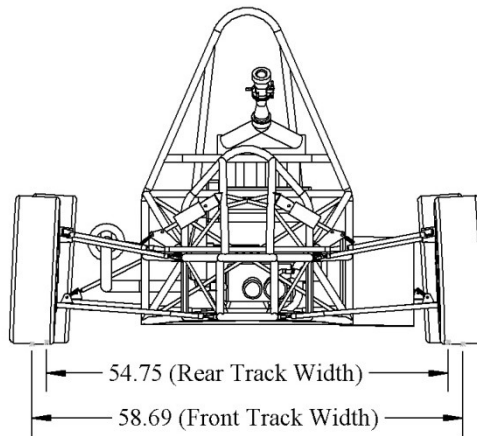


FIGURE 60. 2012 CSULB FSAE showing general dimensions (front view).

TABLE 9. Space frame chassis compartments description

Spaceframe chassis compartments description	
Front cradle	Forward portion of frame, reserved for front suspension, steering system, etc, and provides protection for driver's feet.
Cockpit	Driver's cell, contains main and front roll hoops and side impact structure.
Rear cradle	Rear portion of frame, reserved for rear suspension, engine, drivetrain and intake system, etc.

5.1. Roll Hoops

Main roll hoop is the roll bar located just behind the driver's torso. Front roll hoop is located above driver's legs in proximity to the steering wheel. Main hoop was kept vertical, whereas top portion of front hoop was inclined 15 degrees forward, nearly parallel to the steering wheel. These hoops protect driver's head and hands in any

rollover attitude. Therefore, topmost surface of steering wheel was kept lower than the top surface of front roll hoop. Hoops' height was also selected such that when the driver is seated normally, his helmet is at least 2 inches below the straight line drawn from top of main hoop to top of front hoop as shown in figure 61. These hoops were constructed of single, uncut, continuous round steel tubing of 1 inch diameter. Both of these hoops were constructed of tubes with wall thickness 0.12 inches, however, this study showed the calculated and optimized wall thickness of front roll hoop to be 0.156 inches and for main roll hoop 0.12 inches.

5.2. Main Hoop Bracings

The top round portion of main roll hoop was supported by two main hoop bracings that extend in the rearward direction on both left and right side of main hoop. These bracings form a wide angle of 36 degrees from main hoop which is good for structural point of view. The greater the angle, the better the support would be for main hoop. The other end of these bracing was connected to one of the primary joints of the frame. This was done to make the bracings capable of transmitting all loads from main hoop into the major structure of frame without failing. They were constructed of 1.0" x 0.065" straight round tube. From the lower end of the braces a properly triangulated structure was provided back to the lowest part of the main hoop and the node at which the upper side impact tube meets the main hoop.

5.3. Front Hoop Bracings

The top round portion of front roll hoop was supported by two braces extending in forward direction on both left and right side of front hoop. They protect driver's feet and extend all the way forward to the front bulkhead. These bracings were made of 1.0" x

0.065” straight round tube. At the location where rack and pinion assembly for steering was mounted, additional cross bracings were provided to these bracings since the shock absorbers for front suspension arms were also mounted at the same location.

5.4. Front Bulkhead

The front bulkhead was the forward-most portion of chassis that was actually 8” x 6” rectangular structure constructed of 1” x 0.065” round tubes. It was securely integrated into the frame by means of three frame members on each side of vehicle. One at the top, one at the bottom connecting front bulkhead to front roll hoop, while the third was diagonal brace to provide triangulation. An impact-attenuator was installed forward of front bulkhead to provide protection to the frame and to driver’s feet in the event of an impact.

5.5. Side Impact Structure

It was comprised of three tubes on each side of driver. Upper member connects roll hoops at a height of 11.8 inches above ground. Lower member connects bottom of roll hoops, whereas third member connects roll hoops diagonally for triangulation. Diagonal member was made of 1” x 0.065” tubes and the other two were constructed of 1” x 0.12” tubes. One additional upper frame rail made of 1” x 0.065” tube provided further stiffness and strength to the cockpit.

5.6. Shoulder Harness Attachment Member

This horizontal tube was placed behind the driver’s seat, at a height of 22 in above base of chassis and was constructed of 1” x 0.12” tube. It was not part of hoop bracing and was solely used for shoulder harness mounting to prevent loads being transferred to the bracing.

5.7. Rear Cradle

This compartment mainly comprised of 1" x 0.065" tubes. Two horizontal tubes on each side that connect main hoop bracing to main hoop which were 0.12" thick. The main concept of rear cradle design was to make it tight and compact, just to fit engine, drivetrain and necessary components. For that purpose, SolidWorks CAD model was utilized to find out minimum required dimensions of the rear cradle.

5.8. Tertiary Members

For triangulation, 0.5" x 0.065" tubes were used to provide stiffness and strength to the frame without increasing too much weight to the chassis. Furthermore, this study showed that 0.049" thick tubes could be used to form an optimized structure with less weight as compared to one with 0.065" thick tertiary members.

5.9. Overall Details

As described above, the chassis design was centered around one that takes up minimal space to reduce weight, provide stiffness and to move more weight towards the center of the car. The 0.065" and 0.120" wall tubes were chosen to increase structural rigidity and stiffness of the chassis as well as to increase the safety factor for the driver.

No section of the drivetrain or any moving part were directly exposed to the ground in any attitude of the car, increasing safety and durability. The space just behind cockpit was utilized for intake and exhaust systems. No rear diagonal stiffeners or cross bracings were added behind the cockpit on bottom in order to allow for easy installation of engine. The overall details of Formula SAE vehicle for Cal-State Long Beach 2012 are shown in **Error! Not a valid bookmark self-reference.** Other dimensions showing ergonomics for the driver as per FSAE Rules 2012 are shown in figure 61.

TABLE 10. CSULB FSAE 2012 general details

CSULB FSAE 2012 Details	
WheelBase	68.29 in
Front TrackWidth	58.69 in
Rear TrackWidth	54.75 in
Chassis Length	98.63 in
Chassis Width	28.75 in
Chassis Height	43 in
Center of gravity height	10 in
Chassis Weight	81 lb (optimized)
Chassis Material	SAE 4130 round steel tubes
Suspension Type	Double A-arm with crank-rocker mechanism, coil-springs and dampers
Engine Type	2007 Honda CBR600RR, 4-stroke, 4-cylinder, 599 cc
Drivetrain Type	Chain and Torsen style T1 limited slip differential

For every section of frame where there is a change in overall width, closed loop members were provided to provide stiffness. These include front bulkhead, front and main roll hoops, and another mini-roll hoop behind the cockpit, and finally the rear-most section.

As shown in above analysis results, the maximum displacement is within allowable limit (1 inch) and also the maximum stresses are less than yield strength of material AISI 4130. Hence failure will not be expected to occur anywhere in the system.

As described in the earlier section, torsional stiffness plays a vital role in chassis design, it should be given a consideration. The most effective strategy should include

both the weight reduction and the increase of torsional stiffness. Typical torsional stiffness values for Formula SAE Chassis are in the range of 500-1500 N-m/deg. There are several experimental ways of determining torsional stiffness, this report addressed numerical ways of determining torsional stiffness, using NX. For different load-cases, different values of torsional stiffness have been found. This method would be helpful in future chassis design to increase torsional stiffness.

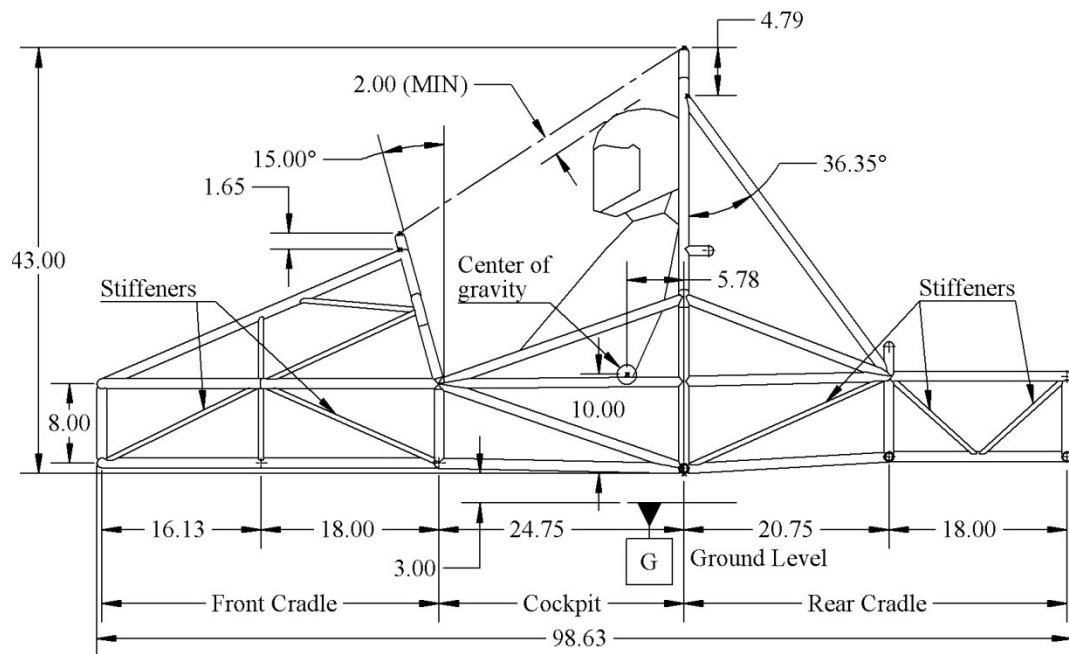


FIGURE 61. Important dimensions complying with FSAE Rules 2012.

CHAPTER 6

CONCLUSION

This report demonstrated the application of numerical solutions, particularly finite element method to solve a realistic design problem represented by a three-dimensional vehicular structure. During the space frame design definitions stage, some difficulties were observed and treated in order to fulfill the design requirements. The frame deflections were minimal for different loading conditions. The only additional requirement was a gusset which was necessary for making front roll hoop safe for its loading condition. Hence the conclusion was that the frame was safe to be used for 2012 model.

The torsional rigidity of the frame is vital in maintaining an accurate alignment and load transfer. The effects were analyzed numerically which opens the door for experimental verification and comparison for the future FSAE frames for CSULB.

Another conclusion related to modeling is that the solid model is not suitable to model tubes with small thickness because of the difficulties on creating the elements. Instead, shell and beam elements were used to optimize the chassis structure. The beam model is the fastest way to compute stresses and conduct optimization on a personal computer. The shell elements required more time for the model development and analysis. A more powerful computer is necessary to run the analysis. However, the

connections are more realistic, so it can describe the physical problem better than the beam model.

Finally, this report showed two ways of optimizing the chassis design. First one focused on maximizing torsional stiffness (K/W method) and the second one focused on minimizing weight using geometric optimization tool present in NX-8 with tube inner radii taken as design variables. The results seem very encouraging as other design variables such as center of gravity, dynamic and manufacturing constraints, can be included in the optimization problems in further research work.

REFERENCES

- [1] Thompson, L. L., Raju, S., and Law, E. H., 1998, "Design of a Winston Cup Chassis for Torsional Stiffness," SAE Technical Paper Series No. 983053, Motorsports Engineering Conference Proceedings, Vol. 1: Vehicle Design and Safety, Dearborn, MI, doi: 10.4271/983053.
- [2] Happian, J.S., 2002, An Introduction to Modern Vehicle Design, Butterworth-Heinemann, Oxford, UK.
- [3] De Oliveira, F., and Borges, J., 2008, "Design and Optimization of a Space frame Chassis," SAE Technical Paper 2008-36-0253, doi:10.4271/2008-36-0253.
- [4] SAE International, "2012 Formula SAE Rules, Section AF4," <http://students.sae.org/competitions/formulaseries/rules/2012fsaerules.pdf>
- [5] Adams, H., 1993, Chassis Engineering: Chassis Design, Building & Tuning for High Performance Handling, Penguin, New York, NY.
- [6] Milliken, D.L., Kasprzak, E.M., Metz, L.D., and Milliken, W.F., 1995, Race Car Vehicle Dynamics, SAE International, Warrendale, PA.
- [7] Costin, M., and Phipps, D., 1974, Racing and Sports Car Chassis Design, Batsford, London, UK.
- [8] Auer, B., McCombs, J., and Odom, E., 2006, "Design and Optimization of a Formula SAE® Frame," SAE Technical Paper 2006-01-1009, doi: 10.4271/2006-01-1009.

